

**AD-A274 768**



2

**PL-TR-93-2115**

**UPPER ATMOSPHERE NEUTRAL  
AND PLAMSA DENSITY MODELING**

**Jeffrey M. Forbes  
Matthew Fox**

**Boston University  
25 Buick Street  
Boston, MA 02215**

DTIC  
S B L  
DEC 15 1993

**31 March 1993**

**Final Report  
25 May 1990-26 May 1993**

**Approved for public release; distribution unlimited**



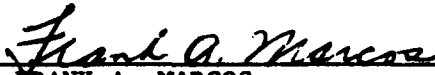
**PHILLIPS LABORTORY  
Directorate of Geophysics  
AIR FORCE MATERIEL COMMAND  
HANSCOM AIR FORCE BASE, MA 01731-3010**

4386 **93-30247**

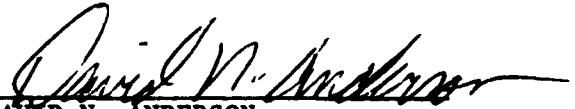


**93 12 14 005**

"This technical report has been reviewed and is approved for publication"



FRANK A. MARCOS  
Contract Manager



DAVID N. ANDERSON  
Branch Chief



WILLIAM K. VICKERY  
Division Director

This report has been reviewed by the ESC Public Affairs Office (PA) and is releasable to the National Technical Information Service (NTIS).

Qualified requestors may obtain additional copies from the Defense Technical Information Center. All others should apply to the National Technical Information Service.

If your address has changed, or if you wish to be removed from the mailing list, or if the addressee is no longer employed by your organization, please notify PL/TSI, Hanscom AFB, MA 01731-3010. This will assist us in maintaining a current mailing list.

Do not return copies of this report unless contractual obligations or notices on a specific document requires that it be returned.

# REPORT DOCUMENTATION PAGE

Form Approved  
OMB No. 0704-0188

Public reporting burden for this collection of information is estimated to average 1 hour per response, including the time for reviewing instructions, searching existing data sources, gathering and maintaining the data needed, and completing and reviewing the collection of information. Send comments regarding this burden estimate or any other aspect of this collection of information, including suggestions for reducing this burden, to Washington Headquarters Services, Directorate for Information Operations and Reports, 1215 Jefferson Davis Highway, Suite 1204, Arlington, VA 22202-4302, and to the Office of Management and Budget, Paperwork Reduction Project (0704-0188), Washington, DC 20503.

<b>1. AGENCY USE ONLY (Leave blank)</b>		<b>2. REPORT DATE</b> 31 March 1993	<b>3. REPORT TYPE AND DATES COVERED</b> Final (25 May 1990-26 May 1993)	
<b>4. TITLE AND SUBTITLE</b>  Upper Atmosphere Neutral and Plasma Density Modeling			<b>5. FUNDING NUMBERS</b> PE 63707F PR 2688 TA 04 WU KC Contract F19628-90-K-0014	
<b>6. AUTHOR(S)</b>  Jeffrey M. Forbes and Matthew Fox				
<b>7. PERFORMING ORGANIZATION NAME(S) AND ADDRESS(ES)</b> Boston University 25 BuickStreet Boston, MA 02215			<b>8. PERFORMING ORGANIZATION REPORT NUMBER</b>	
<b>9. SPONSORING/MONITORING AGENCY NAME(S) AND ADDRESS(ES)</b> Phillips Laboratory 29 Randolph Road Hanscom AFB MA 01731-3010 Contract Manager: Frank Marcos/GPIS			<b>10. SPONSORING/MONITORING AGENCY REPORT NUMBER</b>  PL-TR-93-2115	
<b>11. SUPPLEMENTARY NOTES</b>				
<b>12a. DISTRIBUTION/AVAILABILITY STATEMENT</b>  Approved for public release; distribution unlimited			<b>12b. DISTRIBUTION CODE</b>	
<b>13. ABSTRACT (Maximum 200 words)</b> The neutral density studies described in this report concentrate on specifying tidal aspects of the thermosphere. Firstly, HMEs were used to describe the variations in a database of tidal measurements, providing improved thermospheric specification. Similar techniques were used to derive diurnal and semi-diurnal density corrections to the Grove/MSIS83 model currently used by the AWS. Finally, the variations of satellite-based (SETA) wind and density measurements in the 170-220km high latitude region have been described Plasma modeling work described in this report includes both the development and application of semi-empirical ionospheric models and the application of theoretical models. A simple model was derived for storm-time middle-latitude perturbation in TEC. A simple model of slab thickness was developed leading to a simple successful model of TEC. Slab thickness was also used as a constraint in a new profile formalism that was both validated against an ICS database and extended into a SLIM-like profile model. The PLIM was applied in diagnostic modeling studies to investigate the nature of diurnal double maxima and to derive relationships between ionospheric parameters and satellite-based UV nightglow measurements providing additional ionospheric monitoring at AWS.				
<b>14. SUBJECT TERMS</b> Neutral density variations      Semi-empirical ionospheric models Neutral wind variations      Ionospheric variability Theoretical ionospheric models			<b>15. NUMBER OF PAGES</b> 44	
			<b>16. PRICE CODE</b>	
<b>17. SECURITY CLASSIFICATION OF REPORT</b> Unclassified	<b>18. SECURITY CLASSIFICATION OF THIS PAGE</b> Unclassified	<b>19. SECURITY CLASSIFICATION OF ABSTRACT</b> Unclassified	<b>20. LIMITATION OF ABSTRACT</b> SAR	

## CONTENTS

1. Neutral Density Modeling	1
1.1. Technique for Assimilative Data Analysis	1
1.2. Density Correction Algorithm for Groves/MSIS Model	1
1.3. SETA Density/Wind Analysis and Model Validations	4
2. Plasma Density Modeling	5
2.1. Day-to-Day Variability and Storm-Time Response	6
2.2. A New Global Ionospheric Specification Model	6
2.3. A Diagnostic Modeling Study: Diurnal Twin Peaks	7
2.4. Modeling Ionospheric Nightglow	8
2.5. A Near-Global Model of Total Content	8
2.6. A New Simple Electron Density Profile Description	9
2.7. SKYMAPS: A System for Calibrating 7774Å Imagers and TEC	10
References	12
Appendix	16

DTIC QUALITY INSPECTED I

<b>Accession For</b>	
DTIS GRA&I	<input checked="" type="checkbox"/>
DTIC TAB	<input type="checkbox"/>
Unannounced	<input type="checkbox"/>
Justification	
By _____	
Distribution/	
<b>Availability Codes</b>	
Dist	Avail and/or Special
A-1	

## FIGURE CAPTIONS

- Figure 1. Semidiurnal density amplitude vs. height and latitude at 42°N. 15
- Figure 2. Percent density variation vs. height and local time over the equator during March. 16
- Figure 3. Semidiurnal (top) and diurnal (bottom) density variations as a function of height near the equator, for the 1979 Kwajalein reference atmosphere (solid lines) and densities from the DCORR subroutine. 17
- Figure 4. Daytime densities at 200 km as a result of one-unit  $K_p$  binning and 10° latitude binning over the 20-day observational period. Top: SETA densities (normalized to 200 km) versus  $K_p$  at various geomagnetic latitudes (left) and versus geomagnetic latitude for  $K_p = 4.0$  and 6.0 (right). Middle: Same as top figures, except for the TIGCM at 200 km. Bottom: Same as above, except for the MSISE90 model at 200 km. 18
- Figure 5. Predictions for the storm response in TEC at Hamilton, MA for the 23 November, 1987 storm, compared with the observations (solid line). 19
- Figure 6. (a) Simulation results for the event on 4 February 1984 at Ramey, together with observations. (b) The required vertical drifts ( $V_d$ , positive for upward) at 350 km, induced by a disturbance electric field ( $E_d$  positive for eastward). The dotted vertical lines are used to indicate the temporal correlation between the ionospheric patterns and the enhancement and recovery phases of substorms. 20
- Figure 7. The mean diurnal variations of TEC for all 12 months of 1983 at Ramey, Puerto Rico (solid line), compared to the predictions from models: LMTEC (dashed), Damon-Hartranft (dot-dashed), Bent (dot-dot-dot-dashed) and IRI-90 (long-dashed). 21
- Figure 8. Examples of fits to Millstone Hill IS radar profiles using a double variable Chapman layer formalism. 22

## **PREFACE**

**Contract F19628-90-K-0014 consisted of two main task areas, NEUTRAL DENSITY MODELING and PLASMA DENSITY MODELING. Work completed under these categories are reported below in Sections 1 and 2, respectively.**

## **1. NEUTRAL DENSITY MODELING**

### **1.1 Technique for Assimilative Data Analysis**

In this effort a set of tabulated functions called "Hough Mode Extensions" (HMEs), which represent numerical extensions of classical Hough modes into the viscous regime of the thermosphere, are used to least-squares fit a climatological data base of tidal measurements. The data base consists of monthly average vertical profiles of semidiurnal amplitudes and phases at seventeen radar sites accessing some part of the 80 - 150 km height region. The radars are distributed between 78°S and 70°N latitude, and each one provides measurements of one or more of the following: eastward wind, southward wind, perturbation temperature. As a result of the fitting process, a single complex normalizing coefficient is derived for each month and for each of the four HMEs, designated (2,2), (2,3), (2,4) and (2,5) after their classical Hough function designations. Once the complex coefficients are derived, reconstruction by weighted superposition of the HMEs results in globally continuous specifications of semidiurnal horizontal and vertical wind, temperature, pressure, and density throughout the 80 - 150 km height region. The tidal variations in density, in particular, provide greater accuracy for several aerospace applications. An example of the semidiurnal density amplitudes obtained by this method are depicted in Figure 1. A similar data calibration to numerically-generated tidal functions was performed for the diurnal tide. When combined with the semidiurnal tide, one is able to obtain, for any month and any latitude, the type of percent density variation plots illustrated in Figure 2 for 0° latitude during the month of March.

The methodology described here can also be utilized to derive tidal lower boundary conditions for Thermospheric General Circulation Models (TGCMs), or as a basis for future empirical model development.

A complete description of the above work is contained in the manuscript entitled

**SEMIDIURNAL TIDE IN THE 80 - 130 KM REGION: AN ASSIMILATIVE DATA ANALYSIS**, by J.M. Forbes, A.H. Manson, R.A. Vincent, G.J. Fraser, S.K. Avery, R.R. Clark, R. Schmitter, and D. Kurschner,

which has been accepted for publication in the Journal of Atmospheric and Terrestrial Physics, a preprint copy of which has been delivered to PL/GPIM. In this publication, comparisons are also made with HME coefficients and global tidal fields from the Forbes and Vial [1989] numerical tidal model, and with independent data sets not included in the least-squares fitting process.

### **1.2 Density Correction Algorithm for Groves/MSIS Model**

As a result of the fitting procedure described above, the diurnal and semidiurnal perturbation densities have been fit analytically with Legendre polynomials, and an algorithm (consisting of basically three FORTRAN subroutines) developed which uses these expansions to provide a density correction to the so-called "Groves/MSIS83" density model in operational use by the Air Weather Service. A brief description of the GMSIS83 test program, and the TMOD, DCORR, and DHME subroutines developed under this effort are described below, and are provided in full in the APPENDIX.

### **GMSIS83**

This is a demonstration program which calculates the percent mass density variation about diurnal mean values at various heights and latitudes using (a) the Groves/MSIS83 Model and (b) the DCORR subroutine developed under the present contract. Tables of percent deviation vs. height (80 - 200 km) and local time (0 - 24 hours) are generated at latitudes of 0, 30, and 60 degrees. The intent is to demonstrate use of the DCORR subroutine to those familiar with use of the GROVES subroutine (i.e., the one currently in use by AWS).

In the GMSIS83 code, density variations are first calculated with GROVES. Further below, a similar code appears, except that the percent total mass density variation is provided through a call to TMOD (see below) which subsequently calls DCORR. For altitudes between 145 and 165 km, TMOD provides a linear interpolation between the DCORR results at 145 km, and the Groves/MSIS83 results at 165 km, so that no density discontinuity exists as a result of using DCORR.

It is important to note that DCORR only corrects the tidal *density* variation; that is, when it is implemented in the illustrated fashion, as a correction to the diurnal mean density from Groves/MSIS83, the other parameters (temperature, pressure, etc.) given by Groves/MSIS83 are the diurnal mean values with *no tidal variation whatsoever*. If such variations are required, the Groves/MSIS83 model would have to be called again with the appropriate input parameters.

### **TMOD**

This subroutine provides Groves/MSIS83 densities with "corrected" tidal perturbations between 80 and 145 km, including a smooth merger with Groves/MSIS83 between 145 and 165 km.

### **DCORR**

Subroutine DCORR computes the density correction factor  $\text{dens} = \text{dens} * \text{rc}$  to account for density perturbations due to tides in the 80 to 150 km height regime. The correction factor is determined from Legendre polynomial reconstruction of diurnal ( $n=1$ ) and semidiurnal ( $n=2$ ) harmonics of

perturbation density. This subroutine also provides relative density amplitude ( $\Delta\rho/\rho$ ) and phase (local time of maximum) for the  $n=1$  and  $n=2$  harmonics.

This subroutine contains the normalizing coefficients for the Hough Mode Extension (HME) functions (see Section 1.1), obtained by calls to the DHMEnm (where  $n=1, m=1$  and  $n=2, m=2,3,4,5$ ) subroutines. The coefficients (one set for each month of the year) are provided in data statements. Two options are provided for the semidiurnal tide: (a) from the Forbes and Vial [1989] numerical model; and (b) from least-squares fitting of a global array of wind and temperature data from ground-based radars (see Section 1.1). The latter set, being derived from climatological averages of actual measurements, is the default in the present version of the code. *The table of coefficients derived from data should be updated as more measurements and validation results become available. Operationally, the tidal density correction algorithm should be implemented so that these coefficients can easily be updated.*

#### **DHMEnm where $n=1, m=1$ or $n=2, m=2,3,4,5$**

These subroutines interpolate tables of 6-th order Legendre polynomial coefficients to give the complex HME for perturbation density (percent of mean) of the  $(n,m)$  mode.

A 3.5-inch DOS compatible disk containing the files GMSIS83, GROVES, DCORR, and TMOD were sent to Captain Mark Raffensberger at HQ Air Weather Service/XTX, and to Mr. F.A. Marcos, technical monitor of this contract. Documentation and other descriptive information regarding the methodology of constructing the algorithm were also sent.

The availability of density data distributed over sufficient local times to allow tidal determinations of density within the 80 - 150 km altitude regime, and true validation of the DCORR algorithm, are extremely scarce. One data source can be found in "Kwajalein Reference Atmospheres, 1979", AFGL-TR-79-0241, 24 September, 1979. Here analyses of seventeen high-altitude ROBIN spheres, launched within 48 hours on 19 to 21 July 1978 at Kwajalein, provide data for determination of diurnal and semidiurnal variations in density. The corresponding diurnal and semidiurnal amplitudes are plotted vs height as solid lines in Figure 3, with the DCORR output indicated by dots. The diurnal amplitudes agree reasonably with the Kwajalein values, but the semidiurnal amplitudes are about half of the Kwajalein values. However, one should not put too much weight into the above comparison as it suffers from a number of shortcomings. The Kwajalein data set may not be very representative, and uncertainties exist due to measurement technique and to the Fourier data analysis; however, no information on these possible sources of error are given in the report. On the other hand, real differences may exist at Kwajalein due to longitude effects which are not taken into account in the DCORR formulation. A meaningful evaluation of DCORR requires data

that are not yet in existence. However, the theoretical basis of the present method is reasonably sound, and offers the best possible means of translating a large data base of wind measurements into density variations which are not presently possible to measure on a global scale.

### 1.3 SETA Density/Wind Analysis and Model Validations

Under this effort, satellite-based measurements were utilized to elucidate the latitudinal, local-time, and magnetic activity dependence of winds and densities in the scantily-observed atmospheric region between 170 and 220 km above 45° magnetic latitude. One data set consists of atmospheric densities from high-accuracy (time resolution  $\approx$  5-6 hours) orbital analyses of three Doppler Beacon satellites in orbit during 1973. The perigees of these satellites are generally restricted to 160-180 km, 1200-1400 LST, and geographic latitudes greater than about 45°. Statistical relationships are derived between the density changes and the planetary magnetic index,  $K_p$ , and the five-hour mean of the auroral electrojet index,  $\overline{AE}$ . The former relationships are compared with those derived from the MSISE90 empirical model [Hedin, 1991], which is found to overestimate the rate of increase of density with respect to  $K_p$ .

Another data set consists of densities and cross-track winds from the Satellite Electrostatic Triaxial Accelerometer (SETA) experiment for the 21 March - 9 April, 1979, period, which includes several intervals of elevated magnetic activity. Besides comparing various time series, the data are also binned according to 10° latitude increments and unit increments of  $K_p$  to derive trends. Some typical results include the following, corresponding to average changes in the 45 to 65° magnetic latitude band as  $K_p$  is increased from 1 to 6: (1) For the nightside ( $\approx$  2230 LT), a change in cross-track (nearly zonal) wind from  $25 \pm 25 \text{ ms}^{-1}$  (eastward) to  $-125 \pm 25 \text{ ms}^{-1}$  (westward), and an increase of about 20% in density; (2) For dayside ( $\approx$  1030 LT), a change in cross-track wind from  $25 \pm 25 \text{ ms}^{-1}$  (eastward) to  $125 \pm 25 \text{ ms}^{-1}$  (eastward), and a density increase of 25%. For some individual sudden enhancements in magnetic activity, changes in winds and densities can be more than double the above average values. Comparisons are also made with the NCAR TIGCM (National Center for Atmospheric Research Thermosphere-Ionosphere General Circulation Model) simulation for the complete 20-day interval, and with recent empirical models of densities [Hedin, 1991] and winds [Hedin et al., 1991], with data points in each case derived for the satellite paths, instrument orientations, and sampling rates identical to that of the SETA experiment.

A typical example of the type of comparisons made in this study are provided in Figure 4. Figure 4 illustrates daytime ( $\approx$  1030 LT) density vs.  $K_p$  for several latitudes (left panels) for SETA (top), TIGCM (middle), and MSISE90 (bottom), and also the latitudinal dependences of density (right panels) for the  $K_p = 4$  and  $K_p = 6$  bins. No time delay is assumed in the SETA analysis and

comparisons. Note that the absolute scales for the TIGCM densities are slightly lower, due to the net DC level deficiency of the TIGCM. However, as indicated by the slopes of the curves in the left-hand panels, the relative increase of density with  $K_p$  is very nearly the same for the all three models. The slopes for SETA and TIGCM are more or less independent of latitude up to  $K_p = 4$ . However, for higher  $K_p$  the density increase (slope) is greatest at  $70^\circ$  and least at  $80^\circ$ , for both the TIGCM and SETA analyses. This shows up as maxima in the density vs. latitude plots (right panels) near  $70^\circ$  magnetic latitude, reflecting the maximum in joule heating occurring in the daytime auroral oval. Adiabatic heating and cooling effects connected with the dynamical response of the thermosphere represent alternative processes which can give rise to such maxima (or minima) in the density field [Crowley et al., 1989; Schoendorf et al., 1991]. The MSISE90 model suggests only a slight tendency for maximum density response at  $70^\circ$  latitude for  $K_p \sim 6$ , as indicated in the lower left panel of Figure 4.

A complete description of the work completed under this effort is contained in the manuscript:

**MAGNETIC ACTIVITY DEPENDENCE OF HIGH-LATITUDE THERMOSPHERIC WINDS AND DENSITIES BELOW 200 KM**, by J. M. Forbes, R. G. Roble, and F. A Marcos,

which has been accepted for publication in the *Journal of Geophysical research*, a preprint copy of which has been delivered to PL/GPIM.

## **2. PLASMA DENSITY MODELING**

Ongoing developments and advances in the field of ionospheric modeling come from a variety of sources and motivations. Some of these are in response to the concerns of the user-community, whereby convenient descriptions of ionospheric phenomena are required so that systems can be adjusted to account for both long-term average behavior and short-term perturbations. The main issue addressed in the research presented here is

- can better descriptions be found ?

A number of different analyses are presented herein. Broadly speaking these fit into two categories:

**Data-based** This type of study involves analysis of new or revised data sets, to determine new trends in the data, or to test and validate a new numerical description of data, providing an improved description of variations in the data to the user.

**Model-based** This type of study involves the use of a theoretical ionospheric model used as a diagnostic tool to study particular ionospheric phenomena. This serves both as a validation step on the theoretical model, and at the same times improves our physical understanding of the processes involved, providing in turn a greater level of "predictability" to the user.

### **2.1 Day-to-day Variability and Storm-time Response**

In this effort, the emphasis was to quantify, and where possible, describe, the day to day variability observed in the ionosphere.

Two solar cycles worth of hourly data from both Hamilton, MA (total content, or TEC) and Wallops Is., VA (Nmax) were used as the basis. Slab thickness values were evaluated making only a small correction in local time between the two locations. Firstly, the degree of day-to-day variability was quantified on a monthly basis, and was seen to be as significant as the degree of agreement currently achievable with existing climatological models. Secondly, the level of predictability of these variations were studied, employing the correlation between pairs of these parameters and testing the validity of "persistence" forecasting over various periods. Overall, the bulk of the variations were not accessible by these simple means. Next, it was established that the periods of greatest variability were shown to be geomagnetically active periods, and a separate study of the 400 geomagnetic storms in the database was undertaken. The average storm-time variations were described and related to typical physical processes, but at the same time it was shown that a typical storm and an average storm are quite different. A second model of ionospheric reponse in TEC was developed based on probabilistic considerations of individual storm-time features, and this achieved quite good results, qualitatively, in predicting ionospheric response. An example of predicted ionospheric response is shown in Figure 5, in both the absolute TEC and the percentage deviation from expected behavior.

A complete description of this work is contained in the report

**THE DAY-TO-DAY VARIABILITY OF TOTAL CONTENT, PEAK DENSITY AND SLAB THICKNESS, AND THE IONOSPHERIC RESPONSE TO GEOMAGNETIC STORMS**, by M.W. Fox (1990)

that has been presented to PL/GPIM.

### **2.2 A New Global Ionospheric Specification Model**

It has long been a goal of ionospheric researchers to provide a realistic description of the global ionosphere that is accessible to the user community and responsive to real-time data. Empirical

models of various types (e.g. Llewellyn and Bent, 1973; Rawer and Piggott, 1988) provide convenient summaries of available data yet rely on numerical interpolations in locations and conditions not covered in the initial database. Theoretical models typically involve a large amount of time to generate an ionosphere for a given set of conditions, so are not as accessible.

The Parameterized Real-time Ionospheric Specification Model, or PRISM, involving a significant collaboration of workers, is one attempt to address this situation. Theoretical models appropriate to specific geophysical regions, with the Phillips Laboratory model (Anderson, 1973) being the main component, have been run over a comprehensive grid of conditions, and the resultant variations summarized in a convenient numerical form. Empirical Orthonormal Functions (EOFs) form the basis of electron density profile specification. This simple parameterized model forms the basis for ionospheric description in PRISM. The second stage of PRISM involves a response to available data, whereby the global ionosphere is adjusted according to the departures seen from the parameterized background model and the observations.

A complete description of this work and of the model validation is contained in the report

**PRISM: A PARAMETERIZED REAL-TIME IONOSPHERIC SPECIFICATION MODEL**  
by R.E. Daniell, W.G. Whartenby, L.D. Brown, D.N. Anderson, M.W. Fox, P.H. Doherty, D.T. Decker, J.J. Sojka and R.W. Schunk (1993)

currently under preparation at PL/GPIM.

### **2.3 A Diagnostic Modeling Study : Diurnal Twin Peaks**

This study comprised an investigation of one particular type of diurnal variation in total electron content, namely the diurnal twin-peak. Initially, hourly data from three sites in the Eastern US sector, provided by PL/GPIM, was analyzed to characterize the nature of this phenomenon, describing its frequency, magnitude and variations, in addition to the correlation between the feature at the three locations. It was then established that the feature was both more frequent and of greater magnitude during periods of geomagnetic disturbances, with the twin peaks being related to sub-storm signatures. Case studies suggested that the likely dynamical source for this phenomenon are penetration electric fields, as demonstrated by the time scale for propagation of the effect. Theoretical modeling studies of twin-peak phenomena in turn suggested that a combination of latitude-(equivalently, altitude-)dependent electric fields and chemical loss effects are responsible for the magnitude of the effects observed. Figure 6 shows an example of the modeling results and the nature of the additional vertical drifts/electric fields required to match the observations in a particular case.

A complete description of this work is contained in the report

**DIURNAL DOUBLE MAXIMA IN THE F REGION IONOSPHERE: SUBSTORM-RELATED ASPECTS** by X.Q. Pi, M. Mendillo, M.W. Fox and D.N. Anderson (1993)

that has been delivered to PL/GPIM.

**2.4 Modeling Ionospheric Nightglow**

A new series of instruments are being designed and built for future usage by the Defense Meteorological Satellite Program, DMSP. These will include ultraviolet imaging sensors that will make observations of nightglow both at the nadir and at the earth's limb. The effort conducted at Boston University consisted of applying the Phillips Laboratory ionospheric model (the basis of the PRISM model, described above) at low and middle latitudes to generate a system of calibrations between the observed nightglow intensities and key ionospheric profile parameters below the satellite, thus enabling ionospheric monitoring from DMSP. The ionospheric model was run over a wide grid of conditions (encompassing the grid used for PRISM), but with additional variation of the highly variable vertical  $\mathbf{E} \times \mathbf{B}$  drift patterns at low latitudes in order to build into the system some robustness with respect with day-to-day variability. This model ionosphere was then combined with the neutral atmosphere from MSIS-86 (Hedin, 1987), and the "best available" set of reaction rates that describe the emissions at 1356 Å (through radiative and ion-ion recombination) and 6300 Å (through dissociative recombination). The calibrations were then derived by making multiple point-by-point comparisons between the derived airglow parameters and the parameters of the original ionosphere. Sets of coefficients have been established that relate the observed nightglow intensity both at the nadir and the limb to profile parameters not only in the layer peak but also in the topside and bottomside. These coefficients are simple in nature, allowing a rapid conversion operationally. An error analysis was included, describing the anticipated uncertainties in the results, from (1) internal scatter in the calibrations, (2) propagated errors from the errors in the (nightglow) measurement, and (3) uncertainties in the reaction rates, expressed as partial derivatives.

A complete description of this work is contained in the report

**THE DEVELOPMENT OF CALIBRATIONS FOR IONOSPHERIC PARAMETERS FROM DMSP-BASED NIGHTGLOW OBSERVATIONS** by M.W. Fox, D.N. Anderson and R.E. Daniell (1993)

a draft copy of which has been delivered to PL/GPIM.

**2.5 A Near-Global Model of Total Content**

There is still a large body of the ionospheric user community that relies on simple empirically-derived descriptions of the ionosphere. A number of these models use coefficient-based descriptions of peak parameters to scale a profile of a particular shape, and TEC is derived in turn from the profile. For this effort, a new model for estimating TEC has been developed, along the lines of that proposed by Brown et al. (1991). The model is denoted LMTEC, denoting Low and Middle latitude TEC. The basic premise is that the variations of slab thickness are less than those of foF2, and that much of the complexity of estimating TEC arises from the estimate of foF2. Total content can thus be estimated simply from the coefficient-based (or observed) values of foF2 and a model-based estimate of slab thickness.

Firstly, a slab thickness model needs to be established at lower latitudes. At middle latitudes, the model of Fox et al. (1991) has been used. Also, the variations of slab thickness at lower latitudes in the Anderson (1973) model have been described in the same manner, and the latitude variations of these coefficients in turn summarized numerically. This slab thickness model has been delivered to PL/GPIM.

The next step undertaken was validation of the model against both hourly and monthly mean TEC from a number of sites, with the results compared with those achieved by other models. The predictions for various models of TEC are compared with the monthly mean TEC observed from Ramey, PR, in Figure 7. Generally, comparable results were achieved, though overall, the LMTEC results were systematically the most reliable. This was most evident when uniform peak parameters had been used to drive the various models. It was apparent that a significant source of the numerical discrepancies comes from not precisely estimating the times of the post-sunrise increase and the diurnal maximum. Possibly some improvement would be obtained in LMTEC if higher order terms were introduced into the coefficients that describe the variations of slab thickness. Secondly, a limiting factor at lower latitudes in using LMTEC will be the accuracy of the slab thickness model derived from the Anderson (1973) theoretical ionospheric model. The results suggest that better results may be achieved by using higher order terms, both in the Local Time and latitudinal variations of the model slab thickness.

This work is to be presented as

**A NEAR-GLOBAL MODEL OF TOTAL ELECTRON CONTENT, by M.W. Fox (1993)**

at the Ionospheric Effects Symposium, May 4-6, 1993, in Alexandria, VA, and will subsequently be submitted to Radio Science.

## **2.6 A New Simple Electron Density Profile Description**

A variety of the electron density profile models currently in use rely on specification of the layer peak from some external means (e.g. coefficients) and some parameterized layer shape. However, a recent comparison of a number of ionospheric models currently in use (Brown et al., 1991) showed that no model provided a really good description of the layer shape, as measured by the slab thickness.

For this effort, a new expression for electron density profile shape has been developed. The system scales the profile not only to the peak but also to the value of slab thickness estimated from the model described in the previous section (note also that total content, or a topside density could equally well be used). This additional requirement is necessary to constrain the profile shape. This approach is similar to the SLIM model of Anderson et al. (1987) in that it consists of Chapman layers in the topside and bottomside. However, in this case, the scale height of the Chapman layers are allowed to vary linearly, and this gives rise to a relatively simple (analytic) expression for the layer shape. The name of this model, **DVCHAP**, refers to Double Variable (-scale height) Chapman layers.

The key to specifying the ionosphere in DVCHAP is in knowing the variations of the parameters that describe scale height variations in the topside and bottomside. Two studies were undertaken to examine this. Firstly, the SLIM approach was adopted, and the variations of these parameters in the Anderson (1973) theoretical ionospheric model were described. Secondly, the Millstone IS Radar database of Buonsanto (1989) was examined, and profile residuals were studied as a function of how many ionospheric parameters were known beforehand. Overall, the model is quite successful in describing both theoretical and observation profile shapes. Examples of fits to Millstone Hill profiles are seen in Figure 8.

This work is currently being prepared for publication as

**DVCHAP: A NEW SIMPLE ELECTRON DENSITY PROFILE MODEL**, by M.W. Fox (1993)

and will be submitted to Radio Science.

### **2.7 SKYMAPS : A System For Calibrating 7774A Images And TEC**

For this effort, we examined the feasibility of a system that would permit both the routine monitoring of total electron content from sites with all-sky camera facilities, and that would ultimately provide a means of establishing a calibration for sky-maps (local line-of-sight variations) of total content from the ground-receiver sites in the TISS network. All-sky 7774Å images obtained at Millstone Hill, MA, using the NSF/CEDAR all-sky imaging system run by Boston University (see

e.g. page 258 of Liu, 1989) have been used as a basis.

The questions to answer are

- 1) what are the variations that occur over any given site?
- 2) how can the TEC variations best be recognized against a background that includes both terrestrial and non-terrestrial sources of 7774Å radiation (or how can the system best be trained)?
- 3) what are the best model summaries of the observed features so that recognition of a feature can lead to an update of the "skymap"?

Initially, a database of these observations covering a range of geomagnetic conditions was established. One criterion for the level of "disturbance" in given image was seen to be the amount of scatter about an average intensity vs.  $\sec(\chi)$  relationship. It was next established that in model ionospheres that a reliable calibration exists between  $\Sigma N_e$  (or TEC) and  $\Sigma N_e^2$  (or F-region  $O^+$  radiative recombination). Comparisons then revealed that the Bent model (Llewellyn and Bent, 1973) produced a model ionosphere that was most consistent with the 7774 Å observations. This model also has the advantage of being updated by available data, so would be more appropriate to the proposed TISS-based studies. Unfortunately, in the database, the disturbances seen in the images were auroral in nature, and no trough passages could be detected. For this reason, "training" of the system is waiting on a larger database when F-region effects will be included.



## REFERENCES

- Anderson, D. N., A theoretical study of the ionospheric F region equatorial anomaly, I, Theory, *Planet. Space Sci.*, 21, 409, 1973.
- Anderson, D.N., Mendillo, M. and Herniter, B. A semi-empirical low-latitude ionospheric model, *Radio Science*, 22, 292, 1987.
- Brown, L.D., Daniell, R.E., Fox, M.W., Klobuchar, J.A. and Doherty, P.H. Evaluation of six ionospheric models as predictors of total electron content, *Radio Science*, 26, p. 1007, 1991.
- Buonsanto, M.J., Comparison of incoherent scatter observations of electron density, and electron and ion temperature at Millstone Hill with the International Reference Ionosphere, *J. Atmos. Terr. Phys.*, 51, 441, 1989.
- Crowley, G., Emery, B.A., Roble, R.G., Carlson, H.C., Salah, J.E., Wickwar, V.B., Miller, K.L., Oliver, W.L., Burnside, R.G., and F.A. Marcos, Thermospheric dynamics during September 18-19, 1984; 2. Validation of the NCAR-TGCM, *J. Geophys. Res.*, 94, 16945-16959, 1989.
- Daniell, R.E., W.G. Whartenby, L.D. Brown, D.N. Anderson, M.W. Fox, P.H. Doherty, D.T. Decker, J.J. Sojka and R.W. Schunk, PRISM: A Parameterized Real-time Ionospheric Specification Model, to be submitted to *Radio Science*, 1993.
- Fox, M.W., The Day-to-Day Variability of Total Content, Peak Density and Slab Thickness, and the Ionospheric Response to Geomagnetic Storms, GL-TR-90-0313, Geophysics Laboratory, Hanscom AFB, Bedford, MA, U.S.A., 1990, ADA233294
- Fox, M.W., Mendillo, M. and Klobuchar, J.A. Ionospheric equivalent slab thickness and its modeling applications, *Radio Science*, 26, p. 429, 1991.
- Fox, M.W., D.N. Anderson and R.E. Daniell, Developing a system of calibrations for ionospheric parameters from DMSP-based nightglow observations, to be submitted to *Radio Science*, 1993.
- Hedin, A. E., MSIS-86 thermospheric model, *J. Geophys. Res.*, 92, 4649, 1987.
- Hedin, A. E., Extension of the MSIS thermosphere model into the middle and lower atmosphere, *J. Geophys. Res.*, 96, 1159-1172, 1991.
- Llewellyn, S.K. and Bent, R.B. Documentation and Description of the Bent Ionospheric Model,

**AFCRL-TR-73-0657, Air Force Cambridge Research Lab., Bedford, MA, U.S.A., 1973, AD772733.**

**Liu, C.H. (Ed.) World Ionosphere/Thermosphere Study (WITS) Handbook, Volume 2, Experimental Techniques, December 1989.**

**Pi, X.Q., M. Mendillo, M.W. Fox and D.N. Anderson, Diurnal double maxima patterns in the *F* region ionosphere: Substorm-related aspects, Accepted for publication, *J. Geophys. Res.*, 1993.**

**Rawer, K. and Piggott, W.R. (Eds.) The development of IRI-90 (Proceedings of workshop held at Abingdon, U.K.), *Adv. Space Res.*, 10 (11), 1989.**

**Schoendorf, J., Crowley, G., and R.G. Roble, Neutral density structures in the high latitude thermosphere, *EOS Trans.*, 72, 353, 1991.**

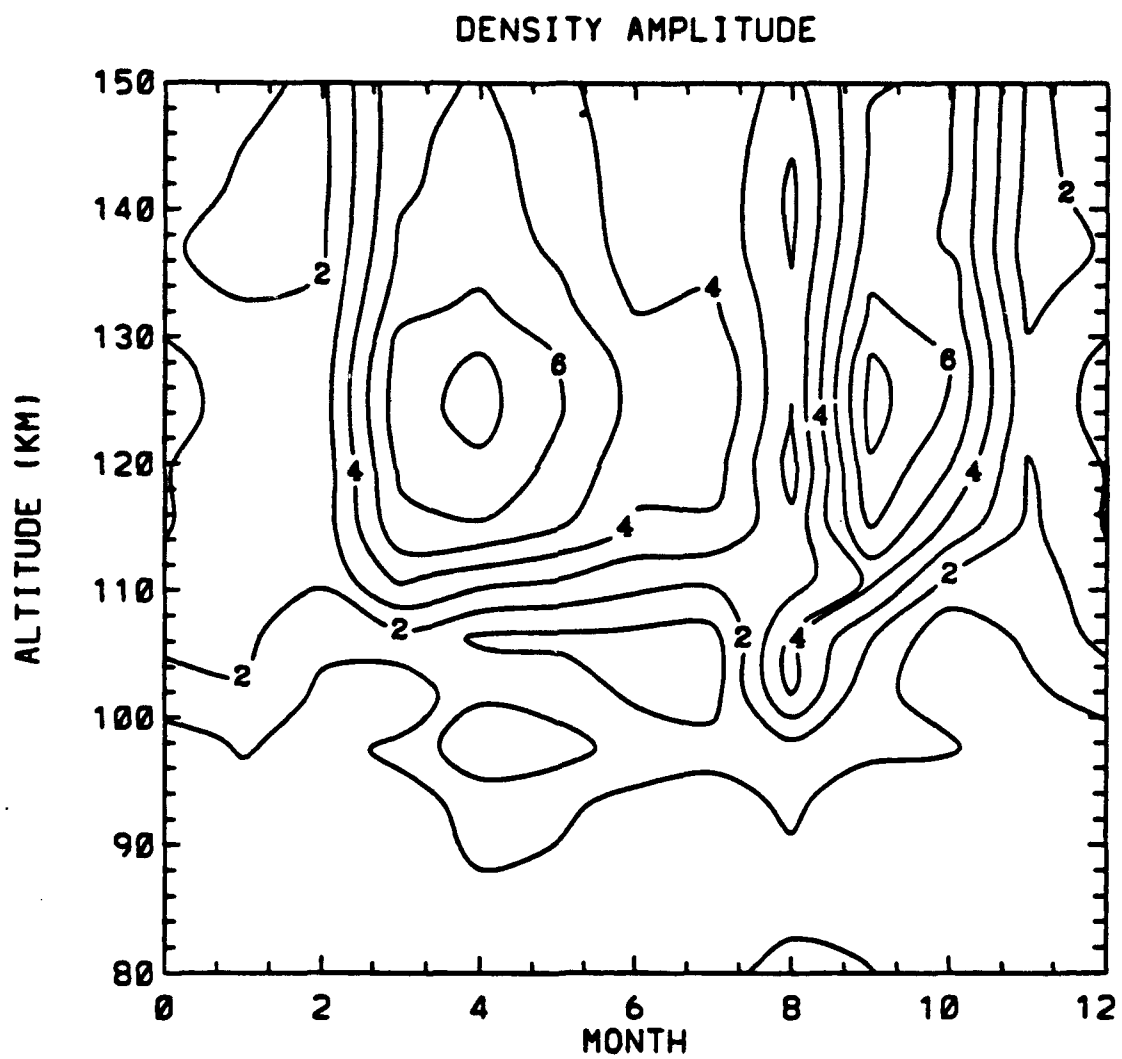


Figure 1

MO = 3

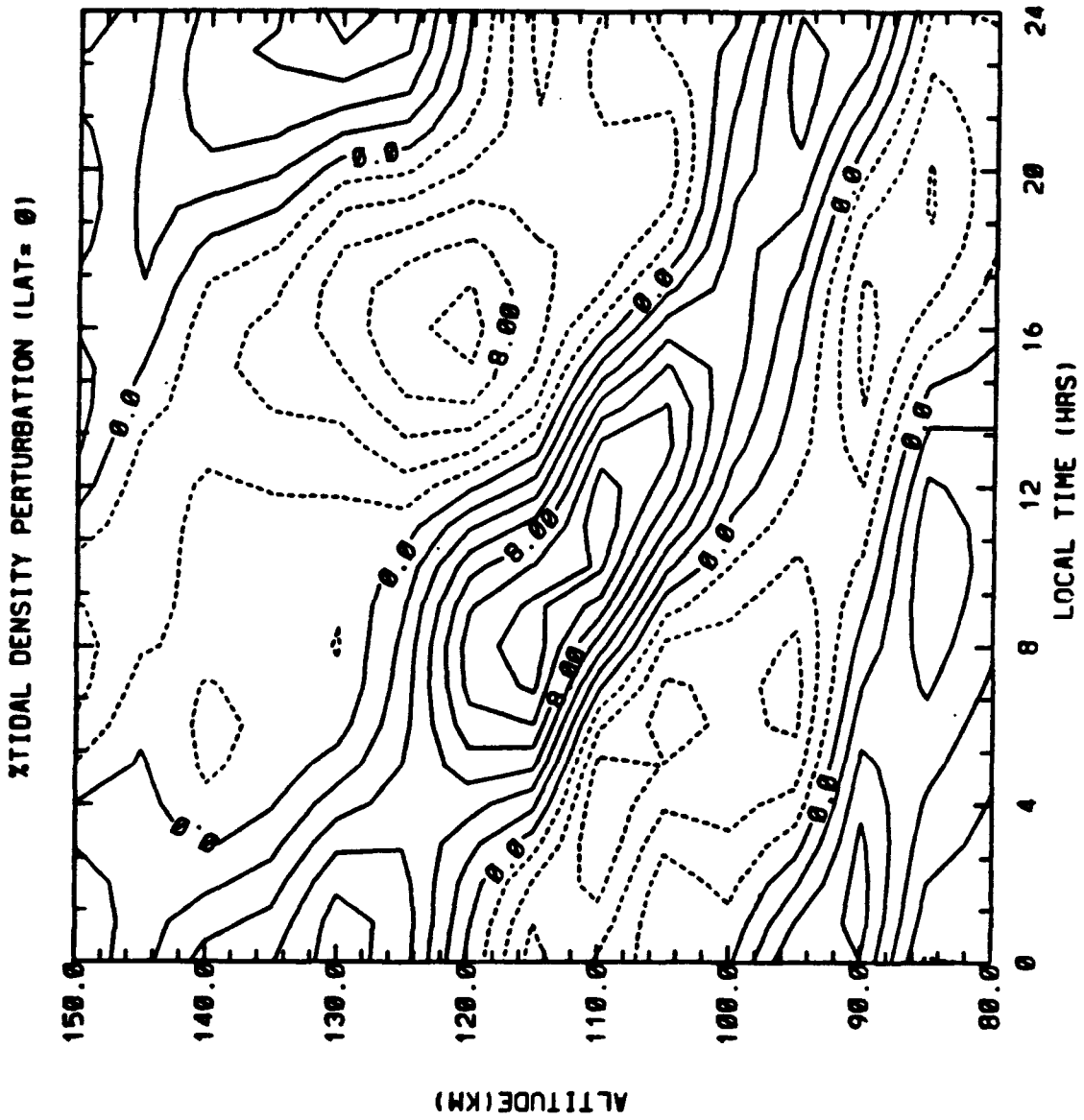


Figure 2

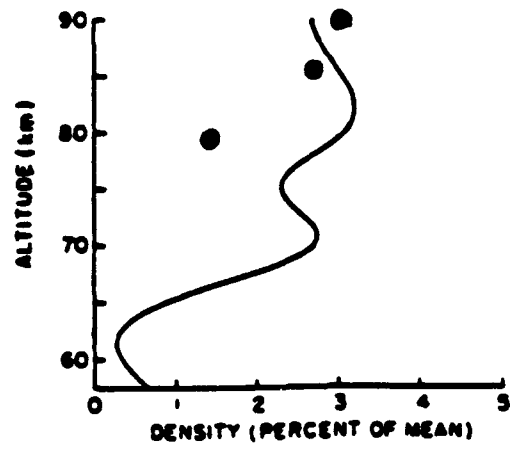
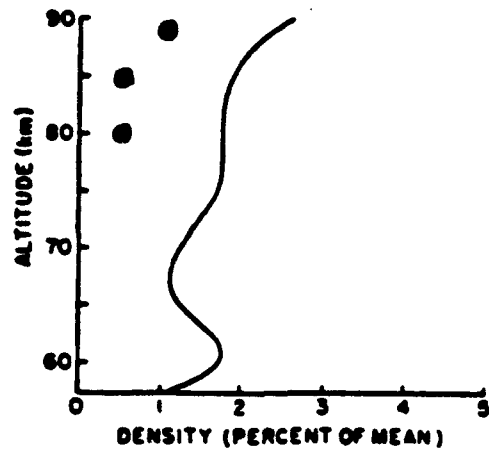


Figure 3

# DAYTIME DENSITY

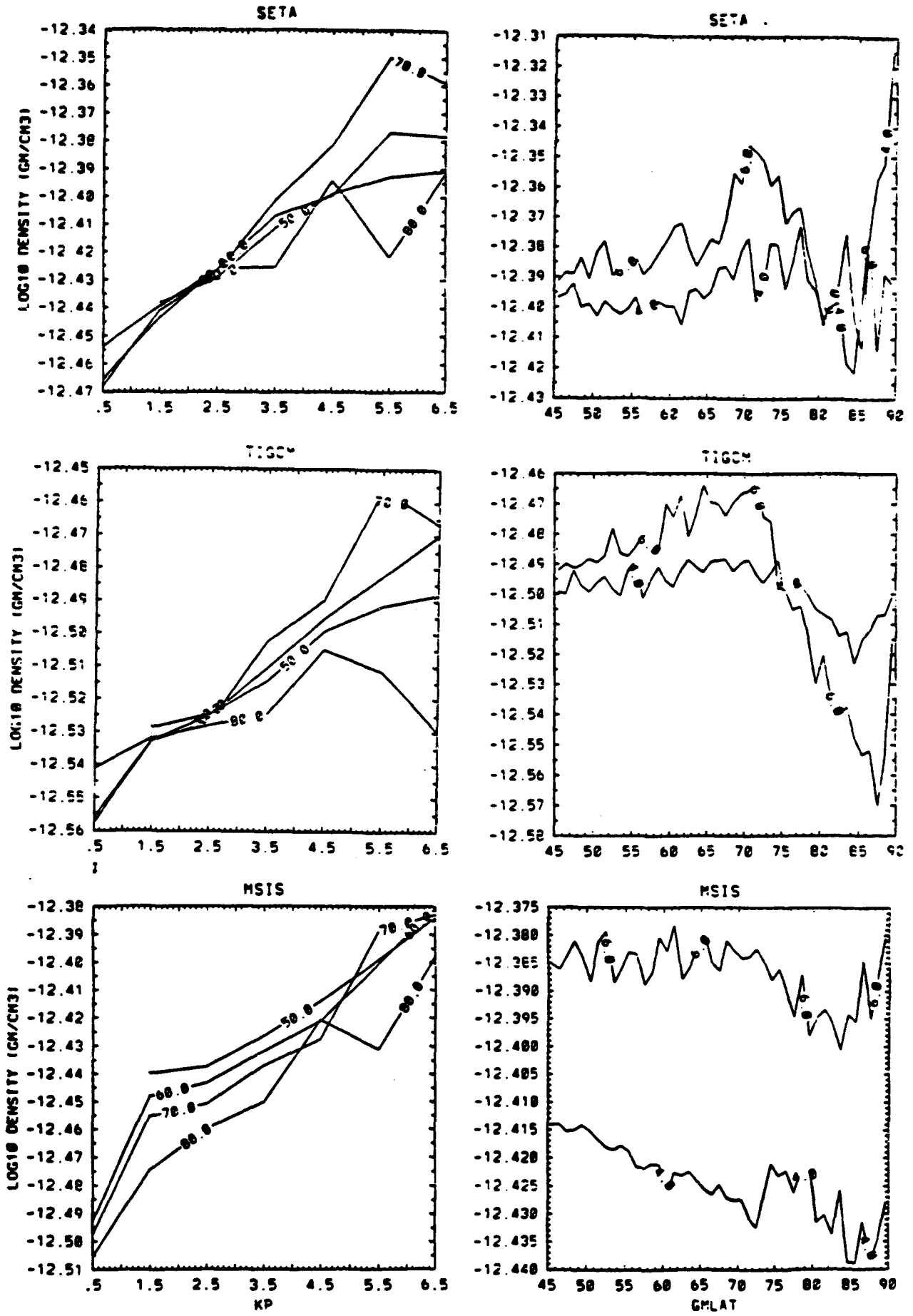
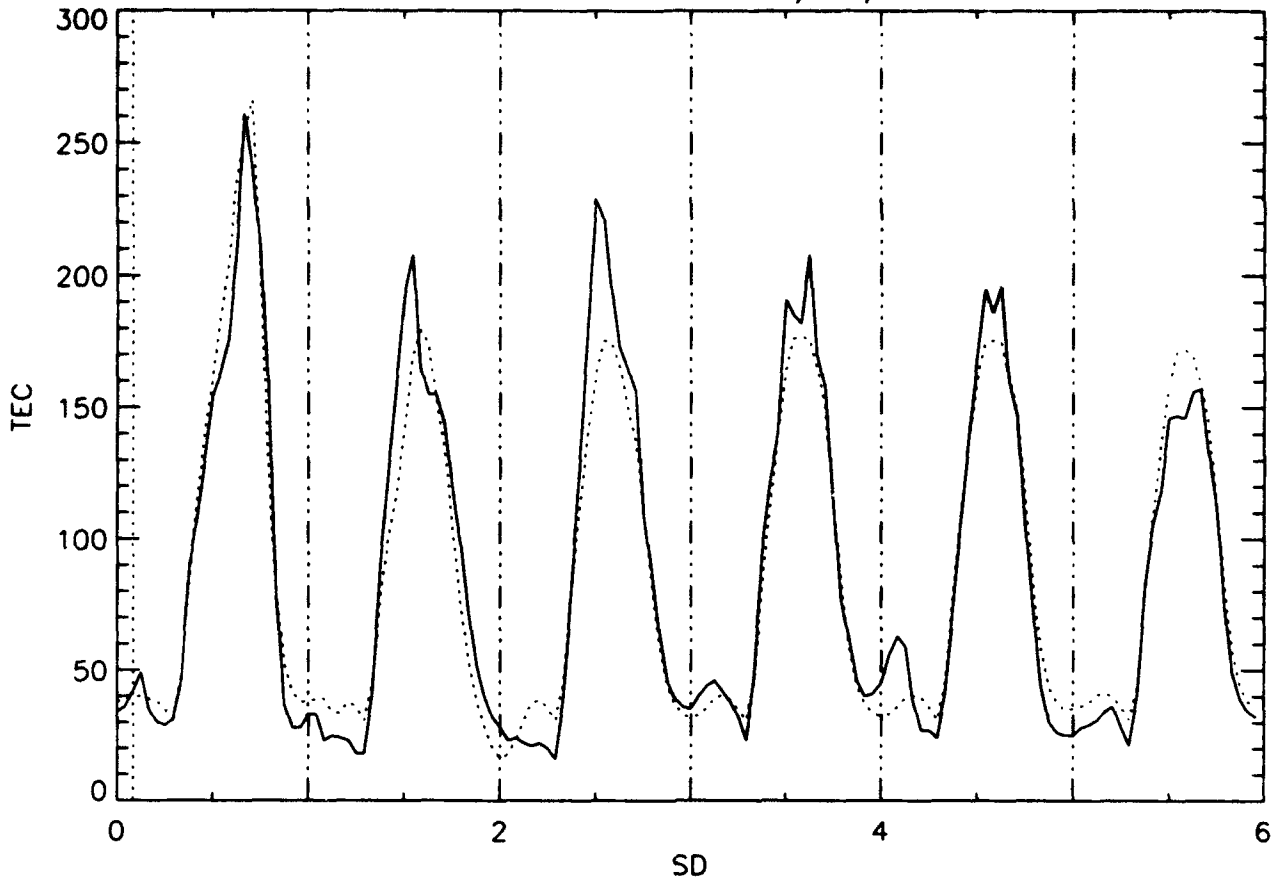


Figure 4  
18

Hamilton TEC from 23/11/1987



% Departures from the mean

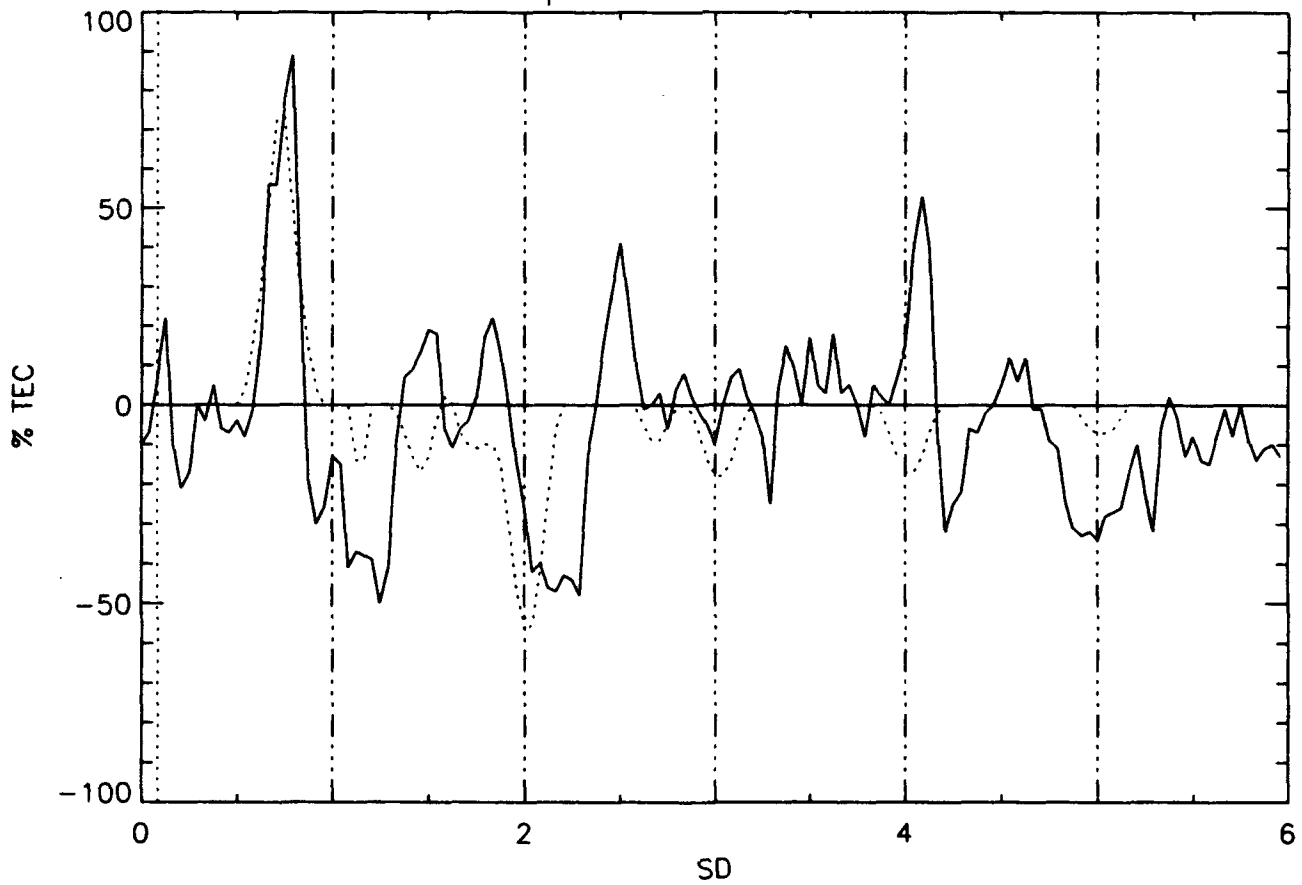


Figure 5  
19

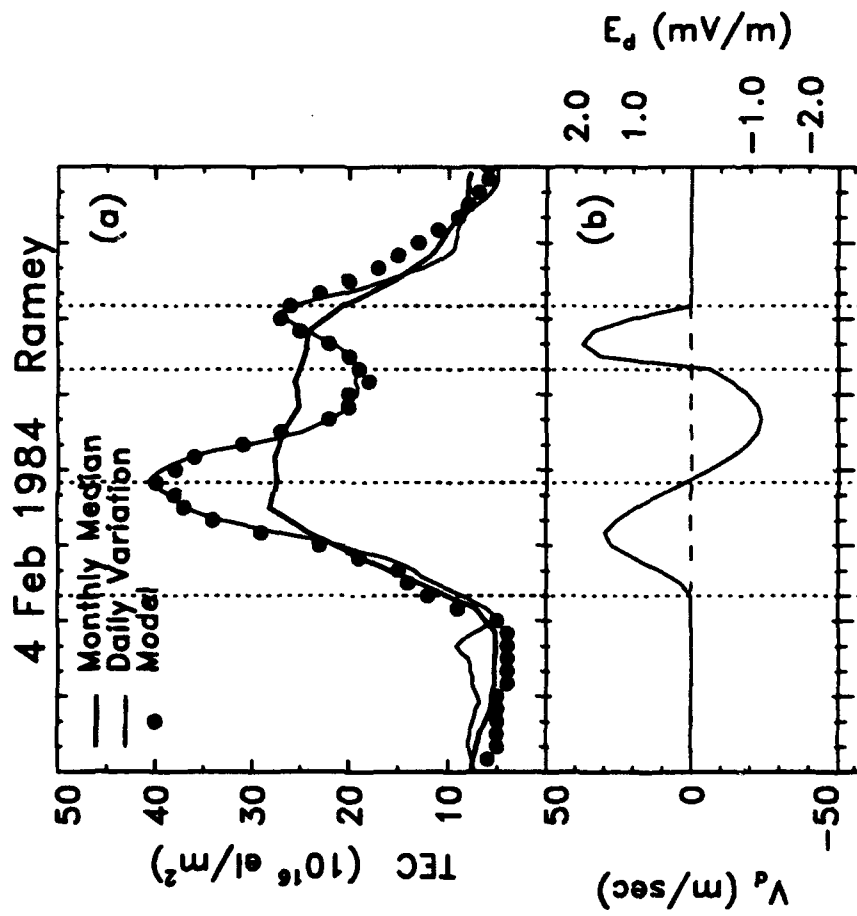


Figure 6

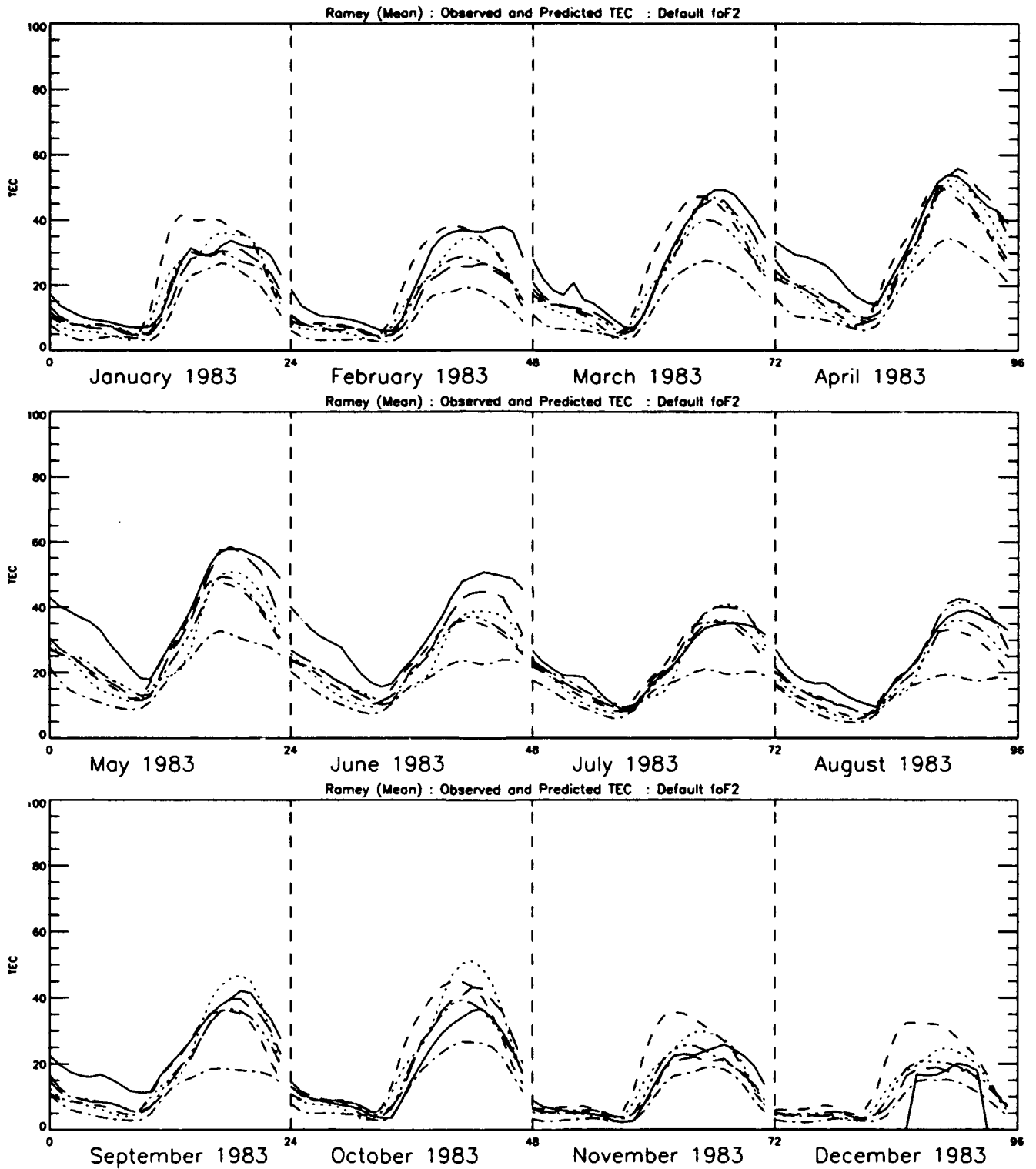


Figure 7

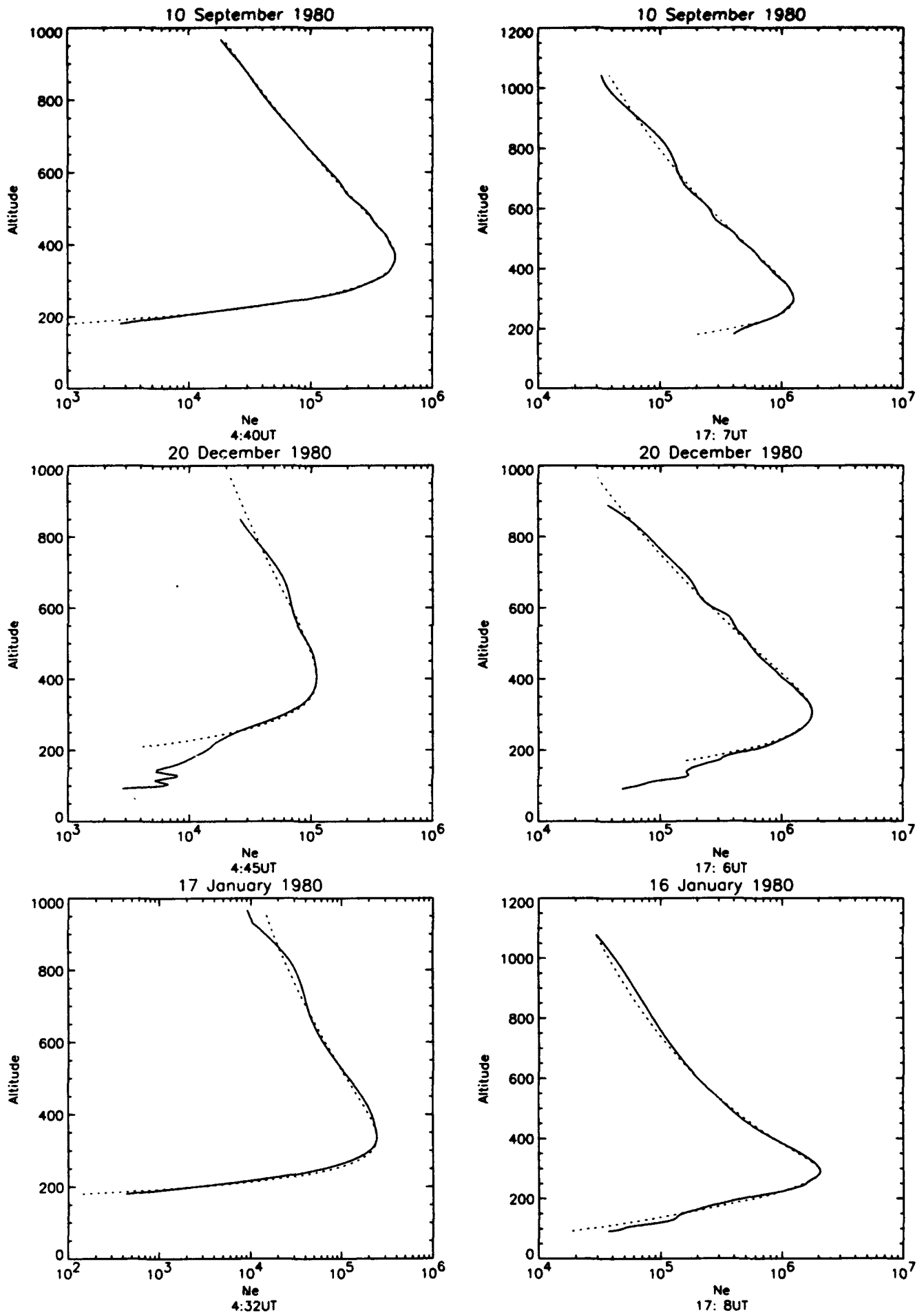


Figure 8

## **APPENDIX**

### **FORTRAN Codes for GMSIS83, DCORR, and TMOD Programs**

SUBROUTINE TMOD

---

```

c
c
subroutine tmod(apf10,itime,pos,zz,dens,temp,press)

c calculate groves/msis densities with "corrected" tidal perturbations
c between 80 and 145 km; smooth merger with groves/msis between
c 145 and 165 km.

real*8 dens(7,50), temp(50), press(50)
real*4 apf10(3), zz(3), pos(3)
integer*4 itime(5)
dimension am(2), ph(2)

c This subroutine is only entered if z.gt.80 and z.lt.165
c It is assumed that zz(1)=zz(2)=altitude=z

xl=pos(1)
t=itime(4)
mo=itime(2)
z=zz(1)

if(z.le.145.) go to 99
c If z.gt.145 interpolate with groves/msis at 165 km

c 1. Calculate tidal correction to groves/msis at 145 km

call dcorr(mo,xl,145.,t,am,ph,rc1)

c 2. Calculate groves/msis tidal correction at 165 km

zz(1)=165.
zz(2)=165.
call setswch(7,0.)
call setswch(8,0.)
call groves(apf10,itime,pos,zz,dens,temp,press)
dmean=dens(1,1)
call setswch(7,1.)
call setswch(8,1.)
call groves(apf10,itime,pos,zz,dens,temp,press)
dt=dens(1,1)
rc2=dt/dmean

c 3. Linearly interpolate to get tidal density correction at altitude z

rc=rc1+(rc2-rc1)*(z-145.)/20.
go to 100

99 continue

call dcorr(mo,xl,z,t,am,ph,rc)

100 call setswch(7,0.)
call setswch(8,0.)
call groves(apf10,itime,pos,zz,dens,temp,press)
dens(1,1)=dens(1,1)*rc

return
end

```

C  
C

PROGRAM GMSIS83

program gmsis83

```
parameter(nt=13, nz=25)
real*8 dens(7,50),temp(50),press(50)
real*4 apf10(3),zz(3),pos(3)
integer*4 itime(5)
dimension am(2), ph(2)
dimension dt(nt),dr(nt,nz),it(nt)
```

```
apf10(1)=120.
apf10(2)=120.
apf10(3)=4.
itime(1)=80
itime(2)=3
itime(3)=21
itime(4)=0
itime(5)=0
zz(3)=1.0
pos(2)=0.0
```

C\*\*\* set switches to turn off semiannual, annual, UT, Ap, longitude, and  
C terdiurnal variations, for comparison with annual mean density  
C perturbations from DCORR.

```
call setswch(3,0.)
call setswch(4,0.)
call setswch(5,0.)
call setswch(6,0.)
call setswch(9,0.)
call setswch(10,0.)
call setswch(11,0.)
call setswch(12,0.)
call setswch(13,0.)
call setswch(14,0.)
```

C  
C Switches 7 and 8 are turned on/off later to turn on/off diurnal and  
C semidiurnal tidal variations in groves/msis.

C  
C \*\*\* The following code calculates the percent total mass density variation  
C about the diurnal mean values at various heights and latitudes using the  
C groves/msis model. Tables of percent deviation vs. height (80-200 km) and  
C local time (0-24 hrs) are generated at latitudes 0, 30, and 60 degrees  
C latitude. Other input parameters for the groves subroutine are given above.

C  
C Further below, a similar code appears, except that the percent total mass  
C density variation is provided by the DCORR subroutine developed by Forbes.  
C This latter code illustrates the implementation of DCORR, which is  
C only valid between 80 and 150 km (hence the tidal switches in groves/msis  
C must be turned on/off depending whether one is outside/inside the 80-150  
C km height regime. In the implementation shown here, DCORR is actually called  
C within subroutine TMOD. For altitudes between 145 and 165 km, TMOD provides  
C a linear interpolation between the DCORR results at 145 km, and the  
C groves/msis results at 165 km, so that no density discontinuity exists as a  
C result of using DCORR.

C  
C It is important to note that DCORR only corrects the  
C tidal DENSITY variation; that is, when it is implemented in the following  
C fashion, as a correction to the diurnal mean density from groves/msis, that  
C other parameters (temp, press, etc.) given by groves/msis are the diurnal  
C mean values with NO tidal variation whatsoever. If such variations are  
C required, the groves/msis model would have to be called again with the  
C appropriate input parameters.

C----- GROVES Version -----

```
300    format(20x,'PERCENT TIDAL DENSITY VARIATION FROM GROVES/MSISS3')
      print 300

      do l=1,3
      xl=(l-1)*30.
      pos(l)=xl
100    format(1x,6hmonth=,i3,3x,4hlat=,f4.0)
      print 100, itime(2),xl
200    format(1x,3hALT)
      print 200

      do i=1,nz
      z=80.+(i-1)*5.
      zz(1)=z
      zz(2)=z

      davg=0.0
      do j=1,nt
      itime(4)=(j-1)*2.
      it(j)=itime(4)
      call setswch(7,1.)
      call setswch(8,1.)
      call groves(apf10,itime,pos,zz,dens,temp,press)
      dr(j,i)=dens(1,1)
      davg=davg+dens(1,1)
      end do
      davg=davg-dens(1,1)
      davg=davg/12.
      do j=1,nt
      dd=dr(j,i)
      dr(j,i)=100.*(dd-davg)/davg
      end do
      end do
      call print(dr,nt,nz,it)
      end do
```

C-----

c \*\*\*\* The "same" code is given below, except DCORR is used to provide the  
c tidal density variations. Lines of code different from the above code are  
c given in UPPERCASE LETTERS.

C-----

C----- DCORR Version -----

```
400    format(20x,'PERCENT TIDAL DENSITY VARIATION FROM DCORR')
      print 400

      do l=1,3
      xl=(l-1)*30.
      pos(l)=xl

      print 100, itime(2),xl
      print 200

      do i=1,nz
      z=80.+(i-1)*5.

      davg=0.0
      do j=1,nt
      itime(4)=(j-1)*2.
      it(j)=itime(4)
```

```

zz(1)=z
zz(2)=z

IF(Z.GT.80.AND.Z.LT.165.) THEN
CALL TMOD(APF10,ITIME,POS,ZZ,DENS,TEMP,PRESS)
ELSE
CALL SETSWCH(7,1.)
CALL SETSWCH(8,1.)
CALL GROVES(APF10,ITIME,POS,ZZ,DENS,TEMP,PRESS)
ENDIF

```

```

dr(j,i)=dens(1,1)
davg=davg+dens(1,1)
end do
  davg=davg-dens(1,1)
  davg=davg/12.
  do j=1,nt
    dd=dr(j,i)
    dr(j,i)=100.*(dd-davg)/davg
  end do
end do

```

```
call print(dr,nt,nz,it)
```

```
end do
```

```

-----C-----
  stop
  end
  subroutine print(dr,nt,nz,it)
  dimension dr(nt,nz),it(nt)
100  format(1x,f4.0,2x,13f5.1)
200  format(1x,4hLST=,2x,13(1x,i2,2x))
300  format(1H1)

  do i=1,nz
  z=80.+(i-1)*5.
  print 100,z,(dr(j,i),j=1,nt)
  end do

  print 200, (it(i),i=1,nt)
  print 300

  return
  end

```

c  
c

SUBROUTINE D CORR

```
subroutine dcorr(mo,xl,z,t,am,ph,rc)
dimension ar(2,7),ai(2,7),p(7),xr(2),xi(2),am(2),ph(2)
complex d11,d22,d23,d24,d25
complex fs(4),fd(4),s(4,12),d(12),xd,xs
common/coeffs/xr,xi
```

c Computes density correction factor dens = dens\*rc to account  
c for density perturbations due to tides in the 80 to 150 km  
c height region. Correction factor is determined from Legendre  
c Polynomial reconstruction of diurnal (n=1) and semidiurnal (n=2)  
c harmonics of perturbation density. This subroutine also returns  
c relative density amplitude (deltarho/rho) and phase (local time  
c of maximum) for the n=1 and n=2 harmonics.

c This April 1992 version includes observationally-determined calibrating  
c coefficients for the HMEs, for month-to-month variations in the  
c n=1 and n=2 harmonics.

c mo = month  
c xl = latitude in degrees  
c z = height in km  
c t = local solar time  
c am = amplitude of relative density perturbation at (mo,xl,z)  
c ph = local time of maximum of relative density perturbation  
c at (mo,xl,z)  
c n = 1 is the diurnal harmonic, with 24-hour period  
c n = 2 is the semidiurnal harmonic, with 12-hour period  
c rc = density correction factor at (xl,z,t) which can be applied to  
c any upper atmosphere density model which does not include tidal  
c effects between 80 and 150 km. In some cases, if a tidal  
c effect is included in such a model above some height z0, then  
c a scheme must be introduced to provide a smooth transition between  
c the two specifications of density variation. This should be done  
c external to the present subroutine.

c\*\*\* hough function values at normalizing latitudes 0, 24, 36, 42  
c degrees for (2,2), (2,3), (2,4), (2,5) modes, respectively \*\*\*  
data h22,h23,h24,h25/1.165,1.091,1.056,1.055/  
data h11/1.0/

c\*\*\*\*\*

c \*\* NOTE \*\*

c THE FOLLOWING TABLES OF COEFFICIENTS ARE THE DRIVERS FOR THE WHOLE DENSITY  
c CORRECTION SCHEME FOR THE 80 - 150 KM REGION. THESE TABLES CAN AND SHOULD  
c BE UPDATED AS MORE DATA BECOMES AVAILABLE. OPERATIONALLY, THE TIDAL DENSITY  
c CORRECTION ALGORITHM SHOULD BE IMPLEMENTED SO THAT THE FOLLOWING COEFFICIENTS  
c CAN BE EASILY UPDATED.

c \*\*\* semidiurnal temps for (2,2), (2,3), (2,4), (2,5) at 100 km  
c from Forbes and Vial (1989) vs. month. These represent a purely  
c theoretical estimate of the coefficients to calibrate the hmes's \*\*\*

c data ((s(i,k),i=1,4),k=1,12)/  
c 1 (2.76,0.5), (1.83,9.3), (3.77,1.4), (7.03,11.4),

```

c      2 (2.18,0.7),      (2.17,8.7),      (4.14,1.1),      (6.17,11.6),
c      3 (1.27,10.8),     (.416,6.5),      (9.28,1.3),      (.402,3.4),
c      4 (1.63,0.2),      (.817,6.4),      (8.11,1.2),      (3.52,6.7),
c      5 (1.87,0.4),      (.932,1.8),      (1.35,0.9),      (4.30,6.1),
c      6 (2.09,0.4),      (1.49,1.7),      (.996,3.1),      (3.40,6.0),
c      7 (1.97,0.7),      (1.85,0.1),      (2.60,6.0),      (4.70,5.8),
c      8 (2.10,0.7),      (2.47,11.7),     (2.12,11.7),     (5.34,6.2),
c      9 (1.22,11.2),     (.473,8.8),      (4.52,0.6),      (3.93,7.0),
c      1 (1.64,0.3),      (.965,4.3),      (6.66,1.3),      (1.14,2.9),
c      2 (2.50,0.3),      (1.29,7.7),      (4.09,0.9),      (5.24,11.9),
c      3 (2.66,0.3),      (2.32,8.5),      (3.03,1.8),      (5.36,11.6)/

```

```

c *** semidiurnal temps for (2,2), (2,3), (2,4), (2,5) at 100 km
c from fit to monthly climatological MLT radar data 80-110 km;
c Incoherent scatter radar data not included in fits *****

```

```

c      data ((s(i,k),i=1,4),k=1,12)/
c      1 (1.97,1.3),      (2.51,2.0),      (1.58,9.3),      (2.24,10.7),
c      2 (1.56,0.3),      (1.14,3.3),      (.72,10.2),      (2.12,11.5),
c      3 (1.55,1.2),      (.87,10.2),      (1.83,11.8),     (.30,1.6),
c      4 (3.07,1.9),      (2.19,10.0),     (1.34,11.4),     (2.15,5.6),
c      5 (1.31,1.8),      (3.07,9.6),      (1.55, 1.5),      (1.56,5.4),
c      6 (1.58,2.0),      (1.25,11.8),     (1.02,10.8),     (.68,5.0),
c      7 (2.00,2.5),      (1.37,10.5),     (.87,1.8),      (.23,7.0),
c      8 (2.53,2.9),      (5.35,10.5),     (1.18,10.5),     (2.11,5.9),
c      9 (2.85,0.6),      (4.28,9.4),      (2.07,3.0),      (2.00,6.3),
c      1 (2.09,2.0),      (2.16,10.3),     (.90,10.2),      (1.06,5.7),
c      2 (2.55,1.8),      (.80,3.2),      (.51,10.4),      (.54,10.4),
c      3 (2.29,2.3),      (1.46,1.2),      (2.46,10.8),     (1.26,10.4)/

```

```

c *** semidiurnal temps for (2,2), (2,3), (2,4), (2,5) at 100 km from
c fit to monthly climatological IS *AND* MLT radar data 80-130 km;

```

```

c      data ((s(i,k),i=1,4),k=1,12)/
c      1 (1.29,5.3),      (2.63,0.3),      (2.00,10.7),     (1.44,10.2),
c      2 (0.42,9.6),      (1.01,10.9),     (1.00,10.7),     (1.08,11.8),
c      3 (1.00,10.4),     (2.88,10.3),     (2.39,11.5),     (0.42,5.9),
c      4 (1.05,1.1),      (4.58,10.3),     (2.13,0.8),      (2.61,5.3),
c      5 (1.12,0.1),      (3.58,10.3),     (1.52,1.2),      (1.69,4.9),
c      6 (.29,1.7),      (2.76,10.6),     (1.53,11.5),     (1.62,4.9),
c      7 (.61,3.1),      (3.25,10.5),     (1.78,1.1),      (1.40,6.1),
c      8 (3.08,3.9),      (5.18,10.5),     (2.72,6.1),      (5.18,10.5),
c      9 (1.50,11.0),     (3.84,8.4),      (3.52,11.2),     (2.39,5.9),
c      1 (1.54,5.2),      (3.63,9.5),      (1.68,11.5),     (1.93,5.0),
c      2 (1.34,4.3),      (1.74,11.1),     (1.49,0.0),      (.47,7.5),
c      3 (1.36,3.9),      (2.28,11.3),     (2.48,11.1),     (.45,10.0)/

```

```

c**** Diurnal calibrating coefficients for (1,1) mode determined from
c Ramey, P.R. and Townesville, Australia wind measurements at 90 km.
c (amp, phase) Amplitude represents tens of meters/sec of diurnal
c eastward wind amplitude at 90 km and 18 degrees latitude; phase is
c local time of maximum eastward wind. k=1,12 corresponds to jan,...dec.

```

```

c      data (d(k),k=1,12)/(2.0,12.),(2.5,12.),(4.0,13.),(2.5,13.),(
c      1 (2.5,13.),(1.5,13.),(2.0,14.),(4.0,14.),(3.0,14.),(1.0,18.),(
c      2 (1.0,8.),(2.0,12.)/

```

```

C*****

```

```

      if(z.lt.80.or.z.gt.150.) go to 99

```

```

      pi=acos(-1.)

```

```

c Define complex HME's at (x1,z):

```

```

call dhme11(z,xl,d11)
call dhme22(z,xl,d22)
call dhme23(z,xl,d23)
call dhme24(z,xl,d24)
call dhme25(z,xl,d25)

```

c Convert normalizing factors for month = mo to complex:

```

do i=1,4
  fs(i)=s(i,mo)
end do
call fxbnd(fs,4,2)
fd(1)=d(mo)
call fxbnd(fd,1,1)

```

c Define diurnal and semidiurnal density variation (complex) at  
c (z,xl,mo):

```

xd = h11*d11*fd(1)
xs = -h22*d22*fs(1) - h23*d23*fs(2)
&      -h24*d24*fs(3) - h25*d25*fs(4)

```

```

xr(1)=real(xd)
xi(1)=aimag(xd)
xr(2)=real(xs)
xi(2)=aimag(xs)

```

c Convert from complex to amplitude and phase  
call ap(xr,xi,am,ph)

c Compute density correction factor at (xl,z,t)

```

rc=1.
do n=1,2
  rc = rc + .01*am(n)*cos((t-ph(n))*float(n)*pi/12.)
end do

```

99 return  
end

```

subroutine ap(xr,xi,am,ph)
dimension xr(2),xi(2),am(2),ph(2)

```

c converts complex form to amplitude and phase (hour LST)

```

pi = acos(-1.)

do n = 1,2
  am(n) = sqrt(xr(n)*xr(n) + xi(n)*xi(n))
  if(am(n).eq.0.0) then
    ph(n) = 0.0
  else
    ph(n) = atan2(xi(n),xr(n))*12./(pi*float(n))
  end if
  if(ph(n).lt.0.0) ph(n) = ph(n) + 24./float(n)
end do

return
end

```

```

subroutine fxbnd(x,k,n)

```

c converts amplitude/phase (LT of maximum) to complex form

```

complex x(4)

```

```

    fn=float(n)
    pi=acos(-1.)

    do 1 i=1,k
    amp=real(x(i))
    phz=aimag(x(i))
    ang=phz*fn*pi/12.
    xr=cos(ang)
    xi=sin(ang)
1    x(i)=amp*cplx(xr,xi)

    return
    end
    subroutine dleg(xl,p)
    dimension p(7),dp(7)
    double precision dp,dxl,cs,fl

```

c computes Legendre polynomial terms through order 6 at latitude = xl

```

    cxl=90.-xl
    dxl = cxl
    cs = dcos(.01745329252*dxl)
    dp(1) = 1.
    dp(2) = cs
    p(1) = 1.
    p(2) = dp(2)
    do i=2,6
    fl=i
    dp(i+1)=((2.*fl-1.)*cs*dp(i)-(fl-1.)*dp(i-1))/fl
    p(i+1) = dp(i+1)
    end do

    return
    end

```

```

    subroutine dhme11(z,xl,d11)

```

```

    complex d11
    dimension cr(15,7),ci(15,7),ar(7),ai(7),p(7)

```

C This subroutine interpolates tables of 6th-order Legendre polynomial  
C coefficients (plus mean) (cr=real; ci=imag), z= 80-150 km (5 km) to  
C give coefficients ar,ai at height = z (km) and latitude = xl (deg)  
C of the complex HME for perturbation density (percent) of the d11 mode.

```

    data ((cr(j,k),k=1,7),(ci(j,k),k=1,7), j=1,5)/
& 0.055742, 0.008325,-0.361614,-0.006649, 0.659095,-0.006027,-0.434787
& ,-0.258680, 0.001143, 0.431332,-0.000285,-0.141635,-0.001914,-0.091767
& ,-0.058174, 0.007919,-0.349165,-0.006532, 1.004046,-0.005700,-0.763388
& ,-0.518292, 0.003793, 1.047003,-0.001672,-0.705835,-0.004603, 0.116936
& ,-0.539064,-0.001736, 1.172848, 0.001360,-0.931498, 0.001963, 0.275171
& ,-0.024488, 0.015533, 0.523313,-0.007622,-1.109352,-0.017836, 0.757128
& ,-0.080068, 0.013846, 0.533738,-0.009426,-0.883046,-0.013050, 0.501360
& , 0.442837, 0.006633,-1.058604,-0.002871, 0.981687,-0.007695,-0.369514
& , 0.253618,-0.012014,-0.425990, 0.007412, 0.157004, 0.011411, 0.062435
& , 0.245779, 0.007735,-0.946197,-0.007577, 1.272626,-0.002400,-0.643730
& /

```

```

    data ((cr(j,k),k=1,7),(ci(j,k),k=1,7), j=6,10)/
& 0.336366,-0.002470,-1.074346,-0.000243, 1.279186, 0.006014,-0.591427
& ,-0.058599, 0.014701,-0.238977,-0.007744, 0.657508,-0.014746,-0.437246
& , 0.243605, 0.007443,-1.290724,-0.003386, 2.083051,-0.008559,-1.226405
& ,-0.290373, 0.010932, 0.621476,-0.007397,-0.474814,-0.009338, 0.123319
& ,-0.001579, 0.013160,-0.485392,-0.011644, 1.079454,-0.007430,-0.735050
& ,-0.355180, 0.001790, 1.497327, 0.001020,-2.240973,-0.004378, 1.302434

```

```

& , -0.137252, -0.012308, 0.468358, 0.011197, -0.604782, 0.006405, 0.308251
& , -0.227223, 0.006073, 1.387512, -0.005586, -2.403057, -0.003632, 1.502747
& , -0.173369, -0.003843, 0.983320, 0.000990, -1.644342, 0.003499, 1.000086
& , -0.061628, 0.006710, 0.735354, -0.002597, -1.453409, -0.007241, 0.959296
& /

```

```

data ((cr(j,k),k=1,7),(ci(j,k),k=1,7), j=11,15)/
& -0.113343, 0.000173, 0.916851, 0.000168, -1.665328, -0.001011, 1.043190
& , 0.022661, 0.008209, 0.186905, -0.004531, -0.498586, -0.008897, 0.368341
& , -0.067469, 0.003385, 0.745517, -0.002250, -1.427778, -0.003014, 0.909452
& , 0.055857, 0.004795, -0.164810, -0.001071, 0.172236, -0.007848, -0.058354
& , -0.021591, 0.004696, 0.547862, -0.002947, -1.129912, -0.002504, 0.737553
& , 0.060800, 0.004317, -0.337485, -0.001998, 0.530214, -0.003967, -0.293422
& , 0.019602, 0.004867, 0.329300, -0.002868, -0.766190, -0.002282, 0.512607
& , 0.046687, 0.003427, -0.382124, -0.002847, 0.661418, -0.000227, -0.384560
& , 0.050399, 0.004739, 0.119047, -0.002744, -0.385148, -0.004707, 0.262498
& , 0.026298, -0.000052, -0.359160, -0.000394, 0.662306, 0.000642, -0.387582
& /

```

```

jz=((z-80.)/5. + .001)
dz=(z-80.-float(jz)*5.)/5.

```

c Modify asymptotic behavior of Legendre polynomial fit at high  
c latitudes to eliminate spurious wiggles.

```

fact=1.0
xm=abs(xl)
if(xl.le.-70.) xl=-70.
if(xl.ge.+70.) xl=+70.
if(abs(xl).ge.70.) fact=exp(-.01*((xl-xm)**2))

```

```

call dleg(xl,p)
xr=0.0
xi=0.0
do 1 k=1,7
ar(k)=cr(jz+1,k)*(1.-dz) + dz*cr(jz+2,k)
ai(k)=ci(jz+1,k)*(1.-dz) + dz*ci(jz+2,k)
xr=xr+ar(k)*p(k)
xi=xi+ai(k)*p(k)
1 continue

```

```

d11=cmplx(xr,xi)*fact

```

```

return
end

```

```

subroutine dhme22(z,xl,d22)

```

```

complex d22
dimension cr(15,7),ci(15,7),ar(7),ai(7),p(7)

```

C This subroutine interpolates tables of 6th-order Legendre polynomial  
C coefficients (plus mean) (cr=real; ci=imag), z= 80-150 km (5 km) to  
C give coefficients ar,ai at height = z (km) and latitude = xl (deg)  
C of the complex HME for perturbation density (percent) of the d22 mode.

```

data ((cr(j,k),k=1,7),(ci(j,k),k=1,7), j=1,5)/
& -0.169341, 0.000000, 0.264998, 0.000000, -0.102197, 0.000000, 0.000000
& , -0.098691, 0.000000, 0.149398, 0.000000, -0.053681, 0.000000, 0.001919
& , -0.361645, 0.000000, 0.475024, 0.000000, 0.000000, 0.000000, 0.000000
& , -0.206671, 0.000000, 0.315332, 0.000000, -0.116397, 0.000000, 0.004485
& , -0.452214, 0.000000, 0.710608, 0.000000, -0.286755, 0.000000, 0.000000
& , -0.235008, 0.000000, 0.349767, 0.000000, -0.135104, 0.000000, 0.022193
& , -0.580654, 0.000000, 0.733212, 0.000000, 0.000000, 0.000000, 0.000000

```

```

& ,-0.285256, 0.000000, 0.356361, 0.000000, 0.000000, 0.000000, 0.000000
& ,-0.683079, 0.000000, 1.049176, 0.000000, -0.381796, 0.000000, 0.017647
& ,-0.279810, 0.000000, 0.484218, 0.000000, -0.288153, 0.000000, 0.085742
& /

```

```

data ((cr(j,k),k=1,7),(ci(j,k),k=1,7), j=6,10)/
& -0.785786, 0.000000, 1.053633, 0.000000, 0.000000, 0.000000, 0.000000
& ,-0.271038, 0.000000, 0.441329, 0.000000, -0.181850, 0.000000, 0.003095
& ,-0.916167, 0.000000, 1.176281, 0.000000, 0.000000, 0.000000, 0.000000
& ,-0.384130, 0.000000, 0.474877, 0.000000, 0.000000, 0.000000, 0.000000
& ,-1.180274, 0.000001, 1.461481, 0.000000, 0.000000, 0.000000, 0.000000
& ,-0.336436, 0.000000, 0.376645, 0.000000, 0.011233, 0.000000, 0.000000
& ,-1.357902, -0.000055, 1.637778, -0.000006, 0.000000, 0.000000, 0.000000
& ,-0.123959, -0.000028, 0.066249, -0.000003, 0.000000, 0.000000, 0.000000
& ,-1.393752, 0.000009, 1.663134, 0.000001, 0.000000, 0.000000, 0.000000
& , 0.227522, 0.000005, -0.376663, 0.000001, 0.000000, 0.000000, 0.000000
& /

```

```

data ((cr(j,k),k=1,7),(ci(j,k),k=1,7), j=11,15)/
& -1.289872, -0.000001, 1.575239, -0.000001, -0.211185, 0.000003, -0.086052
& , 0.409935, -0.000001, -0.737090, -0.000001, 0.301875, 0.000001, 0.034503
& ,-1.162509, 0.000000, 1.362541, 0.000000, 0.000000, 0.000000, 0.000000
& , 0.539921, 0.000000, -0.915434, 0.000000, 0.391622, 0.000000, 0.002363
& ,-1.008992, 0.000000, 1.170860, 0.000000, -0.098578, 0.000000, -0.075953
& , 0.669268, 0.000000, -1.066391, 0.000000, 0.411981, 0.000000, 0.000000
& ,-0.849756, 0.000000, 0.901213, 0.000000, -0.078384, 0.000000, -0.055649
& , 0.777714, 0.000000, -1.162062, 0.000000, 0.386092, 0.000000, 0.000000
& ,-0.705545, 0.000000, 0.685605, 0.000000, 0.044003, 0.000000, 0.000000
& , 0.852396, 0.000000, -1.061791, 0.000000, 0.000000, 0.000000, 0.000000
& /

```

```

jz=((z-80.)/5. + .001)
dz=(z-80.-float(jz)*5.)/5.

```

c Modify asymptotic behavior of Legendre polynomial fit at high  
c latitudes to eliminate spurious wiggles.

```

fact=1.0
xm=abs(xl)
if(xl.le.-70.) xl=-70.
if(xl.ge.+70.) xl=+70.
if(abs(xl).ge.70.) fact=exp(-.01*((xl-xm)**2))

```

```

call dleg(xl,p)
xr=0.0
xi=0.0
do 1 k=1,7
ar(k)=cr(jz+1,k)*(1.-dz) + dz*cr(jz+2,k)
ai(k)=ci(jz+1,k)*(1.-dz) + dz*ci(jz+2,k)
xr=xr+ar(k)*p(k)
xi=xi+ai(k)*p(k)
1 continue

```

```

d22=cplx(xr,xi)*fact

```

```

return
end

```

```

subroutine dhme23(z,xl,d23)

```

```

complex d23
dimension cr(15,7),ci(15,7),ar(7),ai(7),p(7)

```

C This subroutine interpolates tables of 6th-order Legendre polynomial

C coefficients (plus mean) (cr=real; ci=imag), z= 80-150 km (5 km) to  
 C give coefficients ar, ai at height = z (km) and latitude = xl (deg)  
 C of the complex HME for perturbation density (percent) of the d23 mode.

```

data ((cr(j,k),k=1,7),(ci(j,k),k=1,7), j=1,5)/
& 0.000000, 0.006140, 0.000000, 0.000000, 0.000000, 0.000000, 0.000000,
& , 0.000000,-0.011506, 0.000000, 0.034069, 0.000000,-0.026685, 0.000000
& , 0.000000, 0.019873, 0.000000,-0.027559, 0.000000, 0.010279, 0.000000
& , 0.000000,-0.015649, 0.000000, 0.000000, 0.000000, 0.000000, 0.000000
& , 0.000000,-0.003407, 0.000000, 0.000000, 0.000000, 0.000000, 0.000000
& , 0.000000,-0.073662, 0.000000, 0.000000, 0.000000, 0.000000, 0.000000
& , 0.000000, 0.022647, 0.000000, 0.000000, 0.000000, 0.000000, 0.000000
& , 0.000000,-0.088268, 0.000000, 0.000000, 0.000000, 0.000000, 0.000000
& , 0.000000,-0.189464, 0.000000, 0.183542, 0.000000, 0.000000, 0.000000
& , 0.000000, 0.032785, 0.000000, 0.000000, 0.000000, 0.000000, 0.000000
& /

```

```

data ((cr(j,k),k=1,7),(ci(j,k),k=1,7), j=6,10)/
& 0.000000,-0.105329, 0.000000,-0.087378, 0.000000, 0.000000, 0.000000
& , 0.000000, 0.013454, 0.000000, 0.000000, 0.000000, 0.000000, 0.000000
& , 0.000000,-0.347701, 0.000000, 0.650321, 0.000000,-0.410056, 0.000000
& , 0.000000,-0.432722, 0.000000, 0.869166, 0.000000,-0.368488, 0.000000
& , 0.000000,-0.578832, 0.000000, 0.000000, 0.000000, 0.000000, 0.000000
& , 0.000000,-0.195348, 0.000000, 0.000000, 0.000000, 0.000000, 0.000000
& , 0.000000,-0.763669, 0.000000, 0.000000, 0.000000, 0.000000, 0.000000
& , 0.000000, 0.349028, 0.000000,-0.785404, 0.000000, 0.477196, 0.000000
& , 0.000001,-0.711042,-0.000004, 0.000000, 0.000000, 0.000000, 0.000000
& , 0.000004, 0.847518,-0.000007,-1.179172, 0.000010, 0.000000, 0.000000
& /

```

```

data ((cr(j,k),k=1,7),(ci(j,k),k=1,7), j=11,15)/
& 0.000024,-0.837956,-0.000058, 0.974664, 0.000084, 0.007335,-0.000070
& , 0.000031, 0.541760,-0.000082, 0.000000, 0.000000, 0.000000, 0.000000
& , 0.000000,-0.575385, 0.000000, 0.513577, 0.000000, 0.142813, 0.000000
& , 0.000000, 1.085389, 0.000000,-1.418761, 0.000001, 0.000000, 0.000000
& , 0.000019,-0.334993,-0.000047, 0.145217, 0.000069, 0.193542,-0.000057
& , 0.000025, 0.665488,-0.000067, 0.000000, 0.000000, 0.000000, 0.000000
& , 0.000028,-0.143261,-0.000068,-0.075871, 0.000100, 0.155025,-0.000083
& , 0.000035, 0.664996,-0.000094, 0.000000, 0.000000, 0.000000, 0.000000
& , 0.000026,-0.033387,-0.000064,-0.105135, 0.000093, 0.027952,-0.000077
& , 0.000030, 0.598951,-0.000080, 0.000000, 0.000000, 0.000000, 0.000000
& /

```

```

jz=((z-80.)/5. + .001)
dz=(z-80.-float(jz)*5.)/5.

```

c Modify asymptotic behavior of Legendre polynomial fit at high  
 c latitudes to eliminate spurious wiggles.

```

fact=1.0
xm=abs(xl)
if(xl.le.-70.) xl=-70.
if(xl.ge.+70.) xl=+70.
if(abs(xl).ge.70.) fact=exp(-.01*((xl-xm)**2))

```

```

call dleg(xl,p)
xr=0.0
xi=0.0
do 1 k=1,7
ar(k)=cr(jz+1,k)*(1.-dz) + dz*cr(jz+2,k)
ai(k)=ci(jz+1,k)*(1.-dz) + dz*ci(jz+2,k)
xr=xr+ar(k)*p(k)
xi=xi+ai(k)*p(k)
continue

```

1

```

d23=cplx(xr,xi)*fact

```

```
return
end
```

```
subroutine dhme24(z,xl,d24)
```

```
complex d24
dimension cr(15,7),ci(15,7),ar(7),ai(7),p(7)
```

```
C This subroutine interpolates tables of 6th-order Legendre polynomial
C coefficients (plus mean) (cr=real; ci=imag), z= 80-150 km (5 km) to
C give coefficients ar,ai at height = z (km) and latitude = xl (deg)
C of the complex HME for perturbation density (percent) of the d24 mode.
```

```
data ((cr(j,k),k=1,7),(ci(j,k),k=1,7), j=1,5)/
& -0.001112, 0.000000,-0.000112, 0.000000, 0.000000, 0.000000, 0.000000
& , 0.003375, 0.000000, 0.008271, 0.000000,-0.015943, 0.000000, 0.000000
& ,-0.003972, 0.000000, 0.000654, 0.000000, 0.000000, 0.000000, 0.000000
& , 0.005666, 0.000000, 0.011820, 0.000000, 0.000000, 0.000000, 0.000000
& , 0.011253, 0.000000,-0.031639, 0.000000, 0.001761, 0.000000, 0.000000
& , 0.007032, 0.000000, 0.026286, 0.000000,-0.109777, 0.000000, 0.068054
& , 0.009666, 0.000000, 0.004729, 0.000000,-0.038965, 0.000000, 0.000000
& , 0.032353, 0.000000,-0.013593, 0.000000, 0.000000, 0.000000, 0.000000
& , 0.078647, 0.000000, 0.007455, 0.000000, 0.000000, 0.000000, 0.000000
& , 0.053529, 0.000000, 0.176844, 0.000000,-0.414525, 0.000000, 0.187836
& /
```

```
data ((cr(j,k),k=1,7),(ci(j,k),k=1,7), j=6,10)/
& 0.139092, 0.000000, 0.352783, 0.000001,-0.936439, 0.000001, 0.469183
& ,-0.085842,-0.000004, 0.088246,-0.000005, 0.000000, 0.000000, 0.000000
& ,-0.039680,-0.000012, 0.035709,-0.000017, 0.000000, 0.000000, 0.000000
& ,-0.188055, 0.000028,-0.346149, 0.000078, 0.859258, 0.000073, 0.000000
& ,-0.210154, 0.000000,-0.615333, 0.000000, 1.138374, 0.000000, 0.000000
& ,-0.068165, 0.000000, 0.018383, 0.000001,-0.083173, 0.000001, 0.144534
& ,-0.178775,-0.000001,-0.506718,-0.000001, 0.778054, 0.000002, 0.000000
& , 0.066324, 0.000004, 0.232282, 0.000002, 0.000000, 0.000000, 0.000000
& ,-0.142500,-0.000039,-0.113290,-0.000030, 0.149399, 0.000069, 0.094341
& , 0.103712, 0.000056, 0.379078, 0.000006, 0.000000, 0.000000, 0.000000
& /
```

```
data ((cr(j,k),k=1,7),(ci(j,k),k=1,7), j=11,15)/
& -0.065776, 0.000002, 0.152067, 0.000002,-0.428703,-0.000003, 0.347299
& , 0.095648,-0.000006, 0.414288,-0.000001, 0.000000, 0.000000, 0.000000
& ,-0.051485, 0.000000, 0.161603, 0.000000, 0.000000, 0.000000, 0.000000
& , 0.103733, 0.000000, 0.335615, 0.000000, 0.000000, 0.000000, 0.000000
& ,-0.031299, 0.000000, 0.202792, 0.000000, 0.000000, 0.000000, 0.000000
& , 0.086790, 0.000000, 0.247737, 0.000000, 0.000000, 0.000000, 0.000000
& ,-0.011905, 0.000000, 0.209203, 0.000000, 0.000000, 0.000000, 0.000000
& , 0.086470, 0.000000, 0.411871, 0.000000,-0.612001, 0.000000,-0.050880
& , 0.023170, 0.000000, 0.424157, 0.000000,-0.739253, 0.000000, 0.198301
& , 0.077735, 0.000000, 0.324587, 0.000000,-0.447950, 0.000000, 0.000000
& /
```

```
jz=((z-80.)/5. + .001)
dz=(z-80.-float(jz)*5.)/5.
```

```
c Modify asymptotic behavior of Legendre polynomial fit at high
c latitudes to eliminate spurious wiggles.
```

```
fact=1.0
xm=abs(xl)
if(xl.le.-70.) xl=-70.
if(xl.ge.+70.) xl=+70.
if(abs(xl).ge.70.) fact=exp(-.012*((xl-xm)**2))
```

```

call dleg(xl,p)
xr=0.0
xi=0.0
do 1 k=1,7
ar(k)=cr(jz+1,k)*(1.-dz) + dz*cr(jz+2,k)
ai(k)=ci(jz+1,k)*(1.-dz) + dz*ci(jz+2,k)
xr=xr+ar(k)*p(k)
xi=xi+ai(k)*p(k)
continue

```

```
d24=cplx(xr,xi)*fact
```

```

return
end

```

```
subroutine dhme25(z,xl,d25)
```

```

complex d25
dimension cr(15,7),ci(15,7),ar(7),ai(7),p(7)

```

C This subroutine interpolates tables of 6th-order Legendre polynomial  
C coefficients (plus mean) (cr=real; ci=imag), z= 80-150 km (5 km) to  
C give coefficients ar,ai at height = z (km) and latitude = xl (deg)  
C of the complex HME for perturbation density (percent) of the d25 mode.

```

data ((cr(j,k),k=1,7),(ci(j,k),k=1,7), j=1,5)/
& 0.000000,-0.026338, 0.000000,-0.011444, 0.000000, 0.064545, 0.000000
& , 0.000000,-0.011902, 0.000000,-0.007163, 0.000000, 0.000000, 0.000000
& , 0.000000,-0.055506, 0.000000, 0.000000, 0.000000, 0.000000, 0.000000
& , 0.000000,-0.027241, 0.000000, 0.000000, 0.000000, 0.000000, 0.000000
& , 0.000000,-0.123328, 0.000000, 0.000000, 0.000000, 0.000000, 0.000000
& , 0.000000, 0.059905, 0.000000, 0.000000, 0.000000, 0.000000, 0.000000
& , 0.000000,-0.039259, 0.000000,-0.061414, 0.000000, 0.095220, 0.000000
& , 0.000000, 0.257230, 0.000000, 0.121375, 0.000000,-0.549515, 0.000000
& , 0.000000, 0.339623, 0.000000, 0.000000, 0.000000, 0.000000, 0.000000
& , 0.000000, 0.217038, 0.000000, 0.000000, 0.000000, 0.000000, 0.000000
& /

```

```

data ((cr(j,k),k=1,7),(ci(j,k),k=1,7), j=6,10)/
& 0.000000, 0.440520, 0.000002, 0.355003, 0.000003,-0.882318, 0.000007
& ,-0.000001,-0.176003,-0.000003, 0.000000, 0.000000, 0.000000, 0.000000
& ,-0.000024,-0.023348,-0.000067, 0.000000, 0.000000, 0.000000, 0.000000
& , 0.000003,-0.323842, 0.000015,-0.311437, 0.000029, 0.753792, 0.000064
& ,-0.000001,-0.195422,-0.000002, 0.000000, 0.000000, 0.000000, 0.000000
& , 0.000000,-0.069938, 0.000001, 0.106688, 0.000002, 0.000000, 0.000000
& , 0.000000,-0.115362,-0.000002, 0.037199,-0.000003, 0.000000, 0.000000
& , 0.000000, 0.057247, 0.000000, 0.602281, 0.000001,-0.851582, 0.000002
& , 0.000000,-0.012605, 0.000000, 0.412166, 0.000000,-0.593142, 0.000000
& , 0.000000, 0.128748, 0.000000, 0.000000, 0.000000, 0.000000, 0.000000
& /

```

```

data ((cr(j,k),k=1,7),(ci(j,k),k=1,7), j=11,15)/
& 0.000000, 0.066114, 0.000000, 0.000000, 0.000000, 0.000000, 0.000000
& , 0.000000, 0.078923, 0.000000, 0.000000, 0.000000, 0.000000, 0.000000
& , 0.000000, 0.086642, 0.000000, 0.000000, 0.000000, 0.000000, 0.000000
& , 0.000000, 0.023933, 0.000000, 0.084672, 0.000000, 0.000000, 0.000000
& , 0.000000,-0.012868, 0.000000, 0.265220, 0.000000, 0.000000, 0.000000
& , 0.000000, 0.002520, 0.000000,-0.005293, 0.000000, 0.125529, 0.000000
& , 0.000000, 0.065428, 0.000000, 0.000000, 0.000000, 0.000000, 0.000000
& , 0.000000,-0.001040, 0.000000, 0.019997, 0.000000, 0.000000, 0.000000
& , 0.000000, 0.079149, 0.000000, 0.000000, 0.000000, 0.000000, 0.000000
& , 0.000000, 0.006662, 0.000000, 0.000000, 0.000000, 0.000000, 0.000000

```

& /

```
jz=((z-80.)/5. + .001)
dz=(z-80.-float(jz)*5.)/5.
```

```
c Modify asymptotic behavior of Legendre polynomial fit at high
c latitudes to eliminate spurious wiggles.
```

```
fact=1.0
xm=abs(xl)
if(xl.le.-70.) xl=-70.
if(xl.ge.+70.) xl=+70.
if(abs(xl).ge.70.) fact=exp(-.01*((xl-xm)**2))
```

```
call dleg(xl,p)
xr=0.0
xi=0.0
do 1 k=1,7
ar(k)=cr(jz+1,k)*(1.-dz) + dz*cr(jz+2,k)
ai(k)=ci(jz+1,k)*(1.-dz) + dz*ci(jz+2,k)
xr=xr+ar(k)*p(k)
xi=xi+ai(k)*p(k)
1 continue
```

```
d25=cplx(xr,xi)*fact
```

```
return
end
```